Professor MacKenzie
Editorial Office
Atmospheric Chemistry and Physics

22th December 2018

Dear Professor MacKenzie,

Attached please find our revised manuscript entitled "Characterization of VOCs and their related atmospheric processes in a central China city during severe ozone pollution periods" (Manuscript number: acp-2018-397), as well as a point-by-point response to each point raised from the reviewers ("Response to Reviewers"). The revisions to the manuscript are highlighted in blue words in the provided Microsoft Word document.

We would like to express our special thanks to the anonymous reviewers and you for the in-depth reviews. The manuscript has been greatly improved with the valuable suggestion and corrections.

Please do not hesitate to contact me at stevenho@hkpsrl.org or by phone at +00-852-66833994 if you need additional information. Thank you for your time in handling our manuscript.

Sincerely,

Steven S.H. Ho, Ph.D.
Principal Scientist
Division of Atmospheric Sciences
Desert Research Institute
Reno, NV89512,
United States
E-mail: stevenho@hkpsrl.org

Comment and response

Comment 1:

Text for comment 10 is still ambiguous. Please re-write as:
Ten dry days (i.e., no rainfall recorded) were chosen in every month during the period of May - September, 2017 consequently)

Response:

Thanks for the correction, the sentence was revised as

"Ten dry days (i.e., no rainfall recorded) were chosen in every month during the period of May - September, 2017 consequently,"

Comment 2:

The code used to generate air trajectories must be reported.

Response:

The title of Fig.3 was revised as

"Cluster analysis of 48-hour backward trajectories for Zhengzhou in each sampling month using HYSPLIT code, with the start height at 500m altitude and running interval set as 2-hour for each day, percentage of each cluster and covered areas are presented as well."

Comment 3:

Please gloss PMF as "positive matrix factorization".

Response:

The description was revised as

"Factor profiles of major emission sources, namely vehicle emission, coal+biomass burning, solvent usage, oil gas evaporation, petrochemical and biogenic source resolved by positive matrix factorization (PMF) model."

Change list

L105-106 "Ten dry days (i.e., no rainfall recorded) were chosen in every month during the period of May - September, 2017 consequently".

L332-333 "On that day, the ratios of VOCs/NOx at the four sites were all less than 6.5 (ppbC/ppbv)".

Fig. 3 "Cluster analysis of 48-hour backward trajectories for Zhengzhou in each sampling month using HYSPLIT code, with the start height at 500m altitude and running interval set as 2- hour for each day, percentage of each cluster and covered areas are presented as well."

Fig. 15 "Factor profiles of major emission sources, namely vehicle emission, coal+biomass burning, solvent usage, oil gas evaporation, petrochemical and biogenic source resolved by positive matrix factorization (PMF) model."

Marked manuscript

Characterization of VOCs and their related atmospheric processes in a central China city during severe ozone pollution periods

Bowei Li[1], Steven Sai Hang Ho[2,3*], Sunling Gong[1,4*], Jingwei Ni[1], Huairui Li[1], Liyan Han[1], Yi Yang[1], Yijin Qi[1], Dongxu Zhao[1]

[1] *Langfang Academy of Eco Industrialization for Wisdom Environment, Langfang 065000, China*

[2] *Division of Atmospheric Sciences, Desert Research Institute, Reno, Nevada, USA*

[3] *Key Lab of Aerosol Chemistry & Physics, Institute of Earth Environment, Chinese Academy of Sciences, Xi'an 710061, China*

[4] *Center for Atmosphere Watch and Services of CMA, Chinese Academy of Meteorological Sciences, Beijing 100081, China*

*Correspondence to: Steven Sai Hang Ho (stevenho@hkpsrl.org) and Sunling Gong (gongsl@cma.gov.cn)

Revision on: December 22, 2018

Abstract

A five-month campaign (from May to September 2017) was conducted to characterize volatile organic compounds (VOCs) for the first time at four sites in Zhengzhou City, Henan Province, China, where ground level ozone (O_3) concentration shown an increasing trend in recent years. Canister samples were collected for measurement of fifty-seven VOCs, which, along with reactive nitrogen oxides (NOx), are the most important O_3 precursors. During the same period, O_3 and its precursor gases were monitored online simultaneously. The results indicated that the average mixing ratio of total quantified VOCs (Σ_{VOCs} = 28.8±22.1 ppbv) in Zhengzhou was lower than that in the other Chinese megacities, while alkyne was a higher proportion of Σ_{VOCs}. The abundances, compositions and ratios of typical VOCs showed clear spatial and temporal variations. Cluster analysis indicates that air masses from south of Zhengzhou were cleaner than from other directions. The molar ratio of VOCs to NO_x indicated that , in general, O_3 formation was more sensitive to VOCs than NO_x formation in Zhengzhou. The source apportionment was conducted with Positive Matrix Factorization (PMF), and it was found that vehicle exhaust, coal and biomass burning, and solvent usage were the major sources for ambient VOCs at all four sites. From Potential Source Contribution Function (PSCF) analysis, the strong emissions from coal+biomass burning and solvent usage were concentrated in southwest of Shanxi and Henan province. The results of this study gather scientific evidences on the pollution sources for Zhengzhou city, benefiting the Government to establish efficient environmental control measures particularly for O_3 pollution.

1. Introduction

Volatile organic compounds (VOCs) are diverse and reactive chemicals. Vehicle exhausts, fuel combustion and evaporation, and solvent usage are the known major anthropogenic sources of VOCs (Fujita et al., 1994; US EPA, 2000; Fujita, 2001; Borbon et al., 2002) . VOCs play a crucial role in the ground-level ozone (O_3) pollution (Haagen-Smit, 1952; Choek and Heuss, 1987), which has troubled many rapid economy-growth urban cities (Wang et al., 2017b; Nagashima et al., 2017).

Many related studies are thus being conducted globally (Wei et al., 2014; Malley et al., 2015; Ou et al., 2015). In China, the investigations on VOCs including source apportionment, measurement of emission profiles and interpretation of seasonal variations were mainly concentrated in Yangtze River Delta (YRD), Pearl River Delta (PRD) and Beijing-Tianjin (BJT) regions (An et al., 2014; Wang et al., 2014; Chen et al., 2014; Liu et al., 2016; Guo et al., 2017). Limited studies have been conducted in less developed or developing regions (i.e., southwestern and northwestern China) where prominently impacted by biomass burning and with high abundances of toxic and reactive compounds (Li et al., 2014; Li et al., 2017a).

Fifty-seven VOCs, including C_2 - C_{10} alkanes, alkenes, alkynes and aromatics, which greatly contribute to ambient O_3 formation, have been identified and are regularly monitored by Photochemical Assessment Monitoring Stations (PAMS) (US EPA, 1990; Oliver et al., 1996). Due to characteristic structure and reactivity of these compounds, their contributions in O_3 production varies (Carter, 1994); it has been reported that aromatics and alkenes were responsible for most of the weighted reactivity of VOCs (59.4% and 25.8%, respectively) in Pearl River Delta (PRD) region in China (Ou et al., 2015). Consequently, researchers have deduced that reductions of alkenes and aromatics are suitable targets for O_3 control (Wang et al., 2018). In addition, with the variations on energy structure, industrial construction and meteorological conditions (Shao et al., 2011; Wang et al., 2015), major emission sources of VOCs at each city are unique. In less developed cities of Heilongjiang and Anhui, biomass combustion had the highest contribution (40% and 36%, respectively) to the O_3 formation potentials due to high quantity of agricultural activities, while in the developed cities such as Shanghai, Beijing and Zhejiang, solvent usage has become a more important source (Wu and Xie, 2017). Therefore, identification on district emission sources of VOCs is necessary to provide scientific-based information for policy-makers who establish efficient strategies to alleviate O_3 pollution.

In addition to the factors discussed above, non-linear relationships between ambient VOCs, nitrogen oxide (NO_x) and O_3 production such that decreasing tropospheric O_3 is more complex than expected (Lin et al., 1998; Hidy and Blanchard,

2015; Li et al., 2018). Many modeling and field studies showed that photochemical O_3 production in several cities in China such as Guangzhou, Shanghai and Beijing with high levels of NO_x were highly sensitive to VOCs (Shao et al., 2009; Ou et al., 2016; Gao et al., 2017). The sensitivity regime is always varied with time and geographical locations (Luecken et al., 2018). The percentage of VOC-limited regime in North China Plain (NCP) increased from 4% to 6% between 2005-2013, owing to the rapid increases of NO_x emissions (Jin and Holloway, 2015).

Zhengzhou City is an important developing city in the mid-west of the Huanghe-Huaihe river flood plain in China. As the capital city of Henan Province, it is densely populated with more than seven million residents in 2010 (Geng et al., 2013). With the rapid growth of industrial activities, as well as increased vehicle emissions and fuel combustion, air quality in Zhengzhou has deteriorated. The Air quality index (AQI) for 65% of the days in 2013 exceeded the allowable limits of 100 established by the Air Quality Guideline (Chinese Ministry of Environmental Protection, 2012). Particularly O_3 was the major pollutant in summer and over 50% of the days in 2015, the mixing ratio of O_3 exceeded the Grade I standard (100 μg m^{-3}) of daily maximum average 8-hour (DMA8) in Henan (Shen et al., 2017; Gong et al., 2017; Liu et al., 2018). As one of the major precursors of O_3, the study on VOCs is of significance for Zhengzhou, since no related researches are published in peer-reviewed literature. In this work, a comprehensive sampling campaign for VOCs measurement and characterization has been conducted at four monitoring stations during the time period of May - September 2017. The spatial and temporal variations in VOCs in Zhengzhou were determined. The contributions of major emission sources were quantified, and the relationship among O_3-VOCs-NO_x was discussed in details. The results and implications from this study can provide useful guidance for policy-makers to alleviate ozone pollution in Zhengzhou, China.

2. Observation and Methodology

2.1 Sampling site

Based on the density of population distribution, locations of industrial facilities, and the prevailing winds, four sites have been selected for sample collection: Jingkai

community (JK; 113.73°E, 34.72°N), municipal environmental monitoring station (MEM; 113.61°E, 34.75°N), Yinhang school (YH; 113.68°E, 34.80°N) and Gongshui company (GS; 113.57°E, 34.81°N), which are located at the southeastern, southwestern, northeastern and northwestern of Zhengzhou, respectively (Fig. 1). There is a main airport highway and heavy-traffic ring roads approximately 500 m west of JK. Furthermore, the site is at a distance of 2 km from an industrial area, which involves packaging and printing plants, and material distribution factories. It is noteworthy that there are three coal-fired power plants in the urban area of Zhengzhou city. One of the power plants with the highest production was 1.6 km northwest of MEM, and MEM was surrounded by a main road with four traffic lanes, the distance between the nearest traffic light and the sampling site was just 200 m. Both the MEM and YH include a mix of commercial and condensed residential areas, whereas the apartments around YH are more aged. The GS site is surrounded by several manufacturing plants, including pharmaceuticals, materials, foods and machineries.

Ten dry days (i.e., no rainfall recorded) were chosen in every month during the period of May - September, 2017 consequently, to represent a typical air quality condition in a month. Grab samples were collected minute using 3.2 L stainless-steel canisters (Entech Instrument, Inc., Simi Valley, CA, USA), which were pre-cleaned with high purity nitrogen and pressurized to 20 psi. Two samples, one collected at 07:00 with increasing of human activities and another one collected at 14:00 with well-mixed of ambient air, were obtained on each sampling day**.** A total of 400 samples were collected in this study. The chemical analysis was accomplished within two weeks after the collection of samples. Real-time data for trace gases, including SO_2, CO, NO_2/NO_x and O_3, and synchronous meteorological data, such as temperature (T), relative humidity (RH), wind direction (WD) and wind speed (WS), were recorded at each air monitoring station, the message of relevant equipment are listed in Table S1.

2.2 Chemical Analysis

In this study, the measurement of VOCs was based on Compendium Method TO-15, which was established by U.S. EPA (US EPA, 1999). Air in the canister was

concentrated using liquid-nitrogen at -160 °C in a cryogenic pre-concentrator (7100A, Entech Instrument, Inc.). Both CO_2 and H_2O were removed from the transfer line. The air was then thermally desorbed at 120 °C and transferred for analysis to a gas chromatography (GC, 7890A, Agilent Technologies, Santa Clara, CA, USA) coupled with dual detectors, i.e. a mass spectrometric detector (MSD) and a flame ionization detector (FID) (5977E, Agilent Technology). Dual columns were applied for the simultaneous analysis of C_2 - C_{11} hydrocarbons. A PLOT column (15 m, internal diameter of 0.32 mm and film thickness of 3.0 μm) was connected to the FID for detection of C_2 - C_5 NMHCs, whereas C_5 - C_{10} NMHCs, oxygenated VOCs (OVOCs) and halocarbons were separated using a DB-624 column (30 m×0.25 mm inner diameter × 3.0 μm film thickness), which was connected to the MSD. Target compounds were identified with retention time and mass spectra, and quantified with multi-point calibration curve in this study. The standard gas of PAMS (1 ppm; Spectra Gases Inc, NJ, USA) was used to construct the calibration curves for the 57 target VOCs, including 28 alkanes, 11 alkenes, acetylene and 17 aromatics. Detailed information on the target analyses involved in this study and their corresponding linearity of calibration (R^2), measurement relative standard deviation (RSD), method detection limit (MDL), maximum increment reactivity (MIR, Carter, 2010) are presented in Table S2.

2.3 Positive matrix factorization (PMF)

The U.S. EPA PMF 5.0 software was used for source apportionment (Lau et al., 2010; Abeleira et al., 2017; Xue et al., 2017). Due to the complex chemical reactions, the application of PMF in VOCs has to be based on a couple of principles: eliminating species with mixing ratios below MDL and excluding species with high reactivity, except for the source markers (Guo et al., 2011; Shao et al., 2016). Finally, 31 VOC species and NO_2 were chosen for the source apportionment analysis.

In this study, PMF was performed with fifty base runs for each site, results with the minimum Q value (a parameter used to express uncertainties of PMF results) were considered as optimum solutions. In Table S3 the r^2 between observed values and predicted values of selected VOCs and NO_2 are presented for the four sites, the r^2 for

most species (> 80%) were higher than 0.6, compounds with $r^2 < 0.6$ were down weighted when determine factor sources.

During PMF analysis, bootstrap method was used to evaluate stability and uncertainty of the base run solution, setting the minimum correlation coefficient r^2 at 0.6, 100 bootstrap runs were performed, and the results were showing in Table S4, and acceptable results (> 80%) were gained for all the factors.

Three to nine factors were selected to initiate the running of PMF, the Q/Q(exp) for every site at fixed factor size were presented in Table S5. With the increase of factor number, the ratios Q/Q(exp) were declined due to additional factors. When the factor size changing from 3 to 4, 4 to 5, and 5 to 6, the decrement of Q/Q(exp) were larger (~18-25%), while the change was lower than 12% after factors increased to 7, combined with the field conditions, six factors were defined at each site.

2.4 Potential source contribution function (PSCF)

In this trajectory-based study, the probability of air clusters with source concentration higher than a certain value was estimated (Hopke et al., 1995). Briefly, the PSCF value in ij^{th} grid was the ratio of the number of endpoints with higher source concentration relative to the total number of endpoints in ij^{th} grid cell. The criterion value, equal to 75^{th} percentile of the targeted source concentration in this study, was used to verdict whether the value was higher or not. The 48-hour back trajectories was calculated with Hybrid Single-Particle Lagrangian Integrated Trajectory (HYSPLIT) model. Because there are many grid cells with small values, which could result in high uncertainty, a weighting function (Wij) was introduced results (WPSCF) (Polissar et al., 1999). According to average values of end points in each cell, in this case, Wij was presented as below.

$$Wij=\begin{cases}1.0 & nij>30\\ 0.7 & 10<nij\le 30\\ 0.42 & 5<nij\le 10\\ 0.05 & nij\le 5\end{cases}$$

2.5 Estimation of the initial NO_x and VOCs

With the assumption that chemical loss of NO_x and VOCs were mainly due to their reactions with hydroxyl radical (•OH), the initial mixing ratio of NO_x can be calculated with the equation as (Shiu et al., 2007; Shao et al., 2009):

$$[NO_x]=[NO_x]_0 \exp(-k\,[\bullet OH]\,\Delta t) \quad (1)$$

where k stands for the reaction rate between NO_x and •OH. In this study, k was set as the product of the rate constant for NO_2+•OH multiplied by the observed average ratio of NO_2/NO_x during this campaign.

The photochemical age (Δt) can be estimated from the ratio between two compounds, emitted from a common source, but having different reaction rate with •OH. For this case, the photochemical age clock was performed with ethylbenzene (E) and m,p-xylene (X) (Sun et al., 2016).

$$[\bullet OH]\ \Delta t=1/(k_X-k_E)\,[\ln(X_0/E_0)-\ln(C_X/C_E)] \quad (2)$$

which k_x and k_E represent their rate constants with •OH, C_X and C_E correspond to the observed mixing ratios; X_0 and E_0 were their initial concentrations. The X_0/E_0 was estimated from the 5th percentile of the observed ratios at 07:00 in this paper.

The initial mixing ratio of VOC was estimated with the same method as for NO_x (Shiu et al., 2007):

$$[VOC]_0=[VOC]_t \exp(k_i\,[\bullet OH]\,\Delta t) \quad (3)$$

where $[VOC]_t$ was the observed mixing ratio of i^{th} species and k_i was the correspondent rate constant with •OH.

3 Results and discussions

3.1 Meteorological variations and Mixing ratios

Meteorological conditions are important factors that impact both the compositions and levels of VOCs. During the sampling period, the T varied from 15 to 38℃, RH varied from 38 to 100% (Fig. S1), and the dominant winds were northwestern and southeastern (Fig. 2). The air clusters, analyzed by HYSPLIT model, showed moderate differences in each month (Fig. 3). In May, clusters arriving at Zhengzhou demonstrated longer paths, and included six clusters in total, while in June, the length of clusters were shorter. However, the concentration levels and compositions of VOCs were similar in the two months. In May, the largest cluster

(27.2%) was passed over from Yinchuan, a central city in northwest China, then crossing several non-capital cities (i.e., Yanan, Yuncheng and Luoyang) in Shanxi and Sichuan provinces. Such a long-range transport of pollutants has less impact on the air quality of Zhengzhou, as comparable level and similar compositions of VOCs were obtained during the period of May - June. In June, August and September, approximately half of the air trajectories originated from the areas of Henan province, indicating the air pollutants in Zhengzhou were impacted by local factors.

The total concentrations of VOCs (Σ_{VOCs}) are presented in Table 1. The Σ_{VOCs} varied at the four sites, where the highest Σ_{VOCs} and their compositions were not identical across the sampling months as well. In May 2017, the highest Σ_{VOCs} was reported at JK (37.6±22.6 ppbv), followed by GS (31.7±18.7 ppbv), YH (30.1± 16.4 ppbv) and MEM (29.1±15.3 ppbv), while the Σ_{VOCs} values for the month of June, July, August and September were found to be in the order of: GS > JK > MEM > YH, MEM > GS > JK > YH, YH > MEM > JK > GS, and MEM > YH > GS > JK, respectively. This can be attributed to numerous factors that will be explored later in the paper.

Besides the emission sources (to be discussed in Section 3.2), the impacts controlled by meteorological conditions should not be ignored as well. For instance, the prevailing wind in May was northwestern at GS and YH, while the southwestern wind was dominant at JK (Fig. 4). The transport of air pollutants from urban center and industrial plants should be resulted in the highest level of Σ_{VOCs} at JK. In June 2017, the prevailing wind was southeastern at MEM, YH and GS (Fig. 4). The average wind speed at GS (0.74±0.33 m s^{-1}) was lower than that at MEM (1.84±0.94 m s^{-1}) and YH (0.97±0.36 m s^{-1}) (Table 2), indicating poor dispersion conditions at GS. The air pollutants emitted from MEM and YH were more liable resulting in a higher level of Σ_{VOCs} at GS in June. It should be noted that, when Σ_{VOCs} at JK was higher than that of GS, the level at YH was higher than that of MEM, and vice versa. Except for the discriminations between the pollution sources at every site, there may be some other factors (e.g. horizontal and vertical air advection) contribute to it.

Due to the variations of the planet boundary layer (PBL) height, solar radiation

and emission sources, the concentrations of VOCs displayed obvious differences between morning and afternoon time (07:00 LT and 14:00 LT in this study). Compared with morning period, the aromatic compounds showed lower compositions at 14:00 LT (Fig. 5), because of the increased planet boundary layer and the active photochemical reactions, while alkenes always peaked in the14:00 LT. According to the dataset, the increases in alkene compositions (~4.3% uplift) were mainly due to higher contributions of isoprene (~1.4% at morning and 7.6% in the afternoon), which was mainly emitted from biogenic sources and increased exponentially with ambient temperature (Guenther et al., 1993; Guenther et al., 1995).

The average Σ_{VOCs} values in Zhengzhou (28.8±22.1 ppbv) were significantly lower than those in Beijing (65.6 ppbv), Hangzhou (55.9 ppbv), Guangzhou (47.3 ppbv) and Nanjing (43.5 ppbv), and higher than that in Wuhan (23.3±0.5 ppbv) (Table 3). Factors, including population density, industrial activity, fuel composition, local stringent regulations for environmental protection, terrain, and weather are the potential reasons for the differences in VOCs concentrations in those cities. With regard to the weight percentage of major groups (Table 3), the composition of alkanes was the largest in all cities because of their longer lifetimes and widespread sources (Fig. 5), while the composition of aromatics was lower than alkenes in these cities except for Guangzhou. It is well known that aromatics mainly originate from solvent usage and vehicle exhaust in summer. The large amount of shoemaking and shipbuilding industries involving large amounts of solvent usage may be the main reason for the higher composition of aromatics in Guangzhou. In comparison with other four cities, the composition of aromatics in Zhengzhou was the lowest probably due to its less solvent-used manufacturers than in Guangzhou, Hangzhou and Nanjing, and less numbers of vehicles than in Beijing. Alkyne contributes least to VOCs in cities listed in Table 3, with higher level observed in Zhengzhou, where ranked second after Hangzhou. Alkyne typically originates from combustion sources. Zhu et al. (2016) observed that the composition of alkyne in the biomass-burning period could be double of that in the non-biomass burning period (Zhu et al., 2016). As Henan is the largest agricultural province in China and the sampling duration covered the crop

harvest season, the residents often used crop residues as the biofuel for their subsistence and a higher alkyne composition in Zhengzhou was thus resulted.

3.2 Temporal variations

The time series of mixing ratios of NO_x, O_3 and Σ_{VOCs} at every site are shown in Fig. 6. The results showed a distinctive temporal characteristic where lower levels of SO_2, CO, NO_x, O_3 and Σ_{VOCs} were observed in July and August (mid-summer) (Table S6). These results were similar to those obtained for other urban areas worldwide (Cheng et al., 1997; Na et al., 2001; Li and Wang, 2012). Changes in PBL height, human activities, and abundance of •OH were the potential causes for the phenomenon. The occurrence of precipitation, which is usually accompanied with better air dispersion conditions, is also frequent in most areas of China during summer, resulting in decreasing background level of air pollutants. Additionally, a series of effective local policies, such as prohibition of painting and coating in open air and limitations on fuel supply between 10:00 -17:00 LT during hot summer days assisted in suppressing the emissions of VOCs. Meanwhile, many organizations, such as schools, institutes and scattered private workshops, were closed due to summer vacations. Some large-scale industries also stopped manufacturing processes for two weeks during this period. Consequently, the anthropogenic emissions were reduced, which in turn resulted in a decrease in VOCs, SO_2, and NO_x emissions. The reduction of precursor levels and unfavorable photochemical conditions (such as, higher RH) resulted in the lower O_3 levels in July and August.

Beside local emissions, the long-range air mass also had some impacts on relatively lower level of Σ_{VOCs} in July. As illustrated in Fig. 3, different from other months, the air current was originated with the largest portion (*ca*. 88.7%) of clusters from Hubei province, where the average Σ_{VOCs} in its capital city (23.3±0.6 ppbv) (Lyu et al., 2016) was lower than that in Zhengzhou (29.2±23.1 ppbv). In combination with the lower weight percentage of photochemically-reactive aromatics (10.3±4.2%), and the lowest toluene to benzene (T/B) ratio of 1.15±0.99 around this period, it is possible that the cleaner air mass clusters originating from Hubei also contributed to the reduction of Σ_{VOCs} in July.

As demonstrated in Fig. 6, the observed Σ_{VOCs} values at 07:00 LT were often higher than those at 14:00 LT. The accumulation of pollutants during night-time and the temperature inversion in the morning were the most reasonable explanations for this phenomenon. Stronger photochemical reaction during noon-time led to the reduction in atmospheric VOCs. It should be noted that pronounced Σ_{VOCs} were occasionally observed at MEM and GS (Fig. 7), which were potentially ascribed to sharp changes in local emissions and meteorological conditions. Specifically, at MEM, the distinctive increment was always accompanied with obvious increases of alkanes or aromatics (Fig. 7). Since the T and RH were often consistent during the sampling period, the direct gas evaporations should be constant as well. Therefore, the simultaneous increased concentrations of SO_2, CO and NO_x could illustrate the potential impacts from combustion sources, such as emissions from nearby thermal power plant. At GS, the increase of Σ_{VOCs} in June was usually with extremely high levels of aromatics, due to the disturbance from solvent use for building renovation during this period, and the abnormal high levels of Σ_{VOCs} in other months were related to the rising concentrations of C_3-C_4 alkanes, which were mainly originated from consumptions of compressed natural gas (CNG) or LPG (Huang et al., 2015). The results support the possible impact from a gas-fueled power plant located about 1 km southwest of the site (~18% of prevailing western wind at GS during May to September).

It is of interest to note that on the morning of 5th September, acetylene was found in extremely high concentrations (14.7 - 39.4 ppbv). Its mixing ratio in most of the urban areas was < 10 ppbv (Duan et al., 2008; Guo et al., 2012; Louie et al., 2013). 5^{th} September is a festival day for the people who worship their ancestors. A large number of incenses and offerings, made up of wood and paper, were burnt during the festival, resulting in an elevation of acetylene all over the Zhengzhou city (Zhu et al., 2016).

3.3 Spatial variations

The C_2 - C_5 alkanes, acetylene, ethylene, toluene and benzene were the most abundant VOCs detected at all sites (Fig. 8), and the mixing ratios of toluene varied

within a wide range at each site, because of its universal emission sources (e.g., vehicle exhaust emissions and solvent usage) (Barletta et al., 2005; Wang et al., 2014). These chemicals contributed > 60% for Σ_{VOCs} at each site, illustrating strong combustion-related sources in Zhengzhou.

Among the four major organic classes, alkane was the most abundant group as a result of its widespread sources and longevity (Fig. 5), accounted for 52.9%, 62.5%, 53.4%, 53.4% of the total Σ_{VOCs} at JK, MEM, GS, and YH, respectively. The highest composition of alkane was observed at MEM due to the stronger contributions of ethane, iso-pentane, and C_6-C_8 branched alkanes (Fig. S3), which are emitted from light-duty gasoline vehicles (Wang et al., 2017a).

The average Σ_{VOCs} were slightly higher at industrially impacted sites of GS (31.7±28.7 ppbv) and JK (28.6±22.0 ppbv) than those at MEM and YH (Fig. 9). Additionally, the air pollutants related to the combustion processes, such as SO_2 and CO, were marginally more abundant, in western areas of Zhengzhou (GS and MEM) (Fig. 9). Under high levels of VOCs and sufficient supply of NO_x, the highest average mixing ratio of O_3 was observed at GS, followed by YH where even with, which had the lowest VOCs and NO_x, indicating that there are multiple factors, rather than the absolute concentrations, contributing to the formation of the secondary pollutant, O_3 at YH.

In June, the O_3 concentration often exceeded the national standard level of 80 ppbv, i.e., there was severe air pollution during this period. The average mixing ratio of O_3 during daytime (07:00-18:00 LT) in June, 2017 at JK, MEM, YH, and GS were 74.9 ± 39.6 ppbv, 73.5 ± 40.6 ppbv, 73.8 ± 35.7 ppbv, and 88.0 ± 46.1 ppbv, respectively (Table 4). The higher level of O_3 at GS was accompanied with the higher Σ_{VOCs} (39.3 ± 25.4 ppbv). The weight percentage of aromatics (15.6 ± 12.1%) at GS was higher than those at other sites as well, indicating that the painting and other renovation activities at GS was potentially an important factor for its high O_3 level in June. Even though both the Σ_{VOCs} and specifically high O_3 formation potential compounds (such as alkenes and aromatics) at MEM were slightly higher than those at YH (Table 4), the O_3 concentration at MEM was not higher. This could be attributed

to other critical precursors such as NO. NO at MEM (7.72 ppbv) was significantly higher than that at YH (2.57 ppbv) during daytime, indicating that the titration reaction between O_3 and NO was more efficient at MEM.

Because photochemistry producing O_3 occurs over several hours to days, O_3 episodes are attributable not only to local sources but also to regional transports. For example, Streets et al. (2007) reported that with continuous southern winds, the O_3 level in Beijing was 20-30% contributed from its neighboring cities in Hebei. During our study, a typical regional ozone pollution was happened on August 10th at YH (Fig. 6). On that day, the ratios of VOCs/NO_x at the four sites were all less than 6.5 (ppbC/ppbv) (Fig. S4), indicating a regional VOC-control system, and that VOCs are the critical contributors to the formation of O_3 in Zhengzhou. The reductions in Σ_{VOCs} in the afternoons (around 14:00 LT) compared to mornings (around 07:00 LT) may have been due, in part, to chemical loss of VOC as O_3 is formed. The reduction of Σ_{VOCs} and active compounds (i.e., aromatic+alkene) at 14:00 relative to 07:00, 35% and 56% respectively, was least at YH among the four sites (Fig. S4). Based on the wind direction, between 08:00 - 15:00 LT on August 10th, YH was downwind of the other three sites (Fig. S4). All of this confirms that the abnormally high O_3 at YH was caused by the transport of air pollutants from other sites on that day.

3.4 VOCs/NOx ratio

The VOCs/NO_x ratio is often used to distinguish whether a region is VOCs or NO_x limited in O_3 formation. Generally, VOC-sensitive regimes occur when, with VOCs/NO_x ratios are lower than 10 in the morning; NO_x-sensitive regimes occur when VOCs/NO_x ratios are greater than 20 (Hanna et al., 1996; Sillman, 1999). In this study, the mean value of VOCs/NO_x (ppbC/ppbv) were below 5 at all four sites (Fig. 10), and 75% of the data points were < 6, indicating that the O_3 formation was sensitive to VOCs in Zhengzhou, and the reductions on the emissions of VOCs will be a benefit for O_3 alleviation.

The VOCs/NO_x showed differences among the four sites (Fig. 10), with the lowest value at MEM (~3.8) and the highest value at JK (~4.7). The production of O_3 at MEM is more sensitive to VOCs than at JK due to presence of strong NOx

emissions from a thermal-power plant. Approximately 14% of the measured VOCs/NO_x ratios of > 8.0 were found in the NO_x-limited site of JK, resulting from higher VOCs or lower NO_x emissions than at other sites. Both of the mixing ratios and the statistical data showed higher levels of VOCs (with lower NO_x) at GS, where only ~4% of the ratios of > 8.0 was observed, indicating that there must be other factors (unresolved in this study) impacted the variation of O_3 formation regimes.

From the daily variations of VOCs/NO_x ratios (Fig. 10), higher values were observed at 14:00 LT than at 07:00 LT at all four sites, well correlated with less vehicle emissions or more consumption paths for NO_x with stronger light intensity. The increment of VOCs/NO_x at 14:00 LT was more obvious at JK and GS, suggesting that more emission sources of VOCs at daytime, and resulting the O_3 formation system shifting to the transition area in the afternoon.

O_3 formation depends not only on the abundances of precursors (mainly VOCs and NO_x) but also VOCs to NO_x ratio (Sillman, 1999; Pollack et al., 2013). In this research, the mixing ratio of O_3 at 14:00 LT presented a slightly positive trend ($p < 0.05$) with the uplift of VOCs/NO_x at JK (Fig. 11), consistent to the results observed at the megacity of Shanghai (Gao et al., 2017), where the O_3 formation was more sensitive to NO_x when high O_3 levels were observed. Without considering the advection of air parcels, this can be attributed to the increased O_3 production efficiency at high VOCs/NO_x. There were no discernible trends at other sites, possibly due to the counteraction imposed by other uncertain factors.

3.5 Ratios of specific compounds

Ratios of specific VOCs are useful to identify emission sources (Ho et al., 2009; Liu et al., 2015; Raysoni et al., 2017). In order to characterize the differences in the contribution of various sources at each site, ratios of i-pentane/n-pentane and toluene/benzene (T/B) ratios are discussed here.

The ratio of i-pentane to n-pentane can be used to differentiate potential sources such as consumption of natural gas, vehicle emissions and fuel evaporations. In areas heavily impacted by natural gas drilling, the ratios lie in the range of 0.82 - 0.89 (Gilman et al., 2013; Abeleira et al., 2017). Higher values are often reported for

automobiles: in a range of 2.2 - 3.8 for vehicle emissions; and 1.8 - 4.6 for fuel evaporation (McGaughey et al., 2004; Jobson et al., 2004; Russo et al., 2010; Wang et al., 2013), whereas the ratios below unity was found for coal combustion (0.56 - 0.80) (Yan et al., 2017).

In this study, i-pentane and n-pentane were highly correlated (R^2=0.87 - 0.94) throughout the whole sampling campaign (Fig. 12), indicating constant pollution sources for these two compounds. The highest ratio of i/n-pentane was found at JK (2.59±0.45), which was comparable to the value of 2.93 reported in a Pearl River Tunnel (Liu et al., 2008), thus indicating strong impacts from traffic-related sources. The average ratio at MEM was 2.31±0.68, higher than the character ratios of coal combustion, reasonably due to the observation site presented at upwind position of the thermal power plant. And frequent idling may cover up the contribution from coal combustion, reflecting the impact of traffic emissions. The average ratios at YH (1.94 ±0.57) and GS (1.63±0.51) were lower than those at the above two sites, suggesting the comparatively stronger contribution from coal burning.

Tunnel and roadside researches indicates that T/B ratio varies within the range of 1 - 2 when the atmosphere is heavily impacted by vehicle emissions (Wang et al., 2002; Tang et al., 2007; Gentner et al., 2013; Huang et al., 2015). The ratio of < 0.6 was ascribed to other sources such as coal combustion and biomass burning (Tsai et al., 2003; Akagi et al., 2011). The industrial activity would be more dominant when the T/B ratio is greater than 3 (Zhang et al., 2015).

In this study, the correlation between benzene and toluene was fairly well at all the sites (R^2=0.70-0.74), except for YH (R^2=0.41) (Fig. 14), suggesting the similar sources for benzene and toluene at JK, MEM and GS, while more complex such as variable wind direction at YH. The average ratios of T/B were lied within the range of 1.64-2.29, which were scattered around the character ratio of 2 for vehicle exhaust, illustrating the significance of vehicle emissions at the four sites. Specifically, at JK, MEM and YH, most of T/B ratios were distributed between 0.6 and 3, which were corresponding to character ratios for coal or biomass burning and industrial activities respectively. These reflected the mixture impacts from mobile source and

coal/biomass burning at these three sites. However, more values were greater than 3 at GS, suggesting more frequent disturbance from industrial activities at this site.

The T/B ratios at 14:00 LT were lower than at 07:00 LT (Fig. 15). The reaction rate constant of toluene (5.63×10^{-12}cm^{3}molecule^{-1}s^{-1}) with •OH is higher than that for benzene (1.22×10^{-12}cm^{3}molecule^{-1}s^{-1}), indicating more rapid consumption of toluene from photochemical reactions and thus resulting in lower T/B ratios at 14:00 LT, all else being equal. The emission strength of mobile source is often weaker at 14:00 LT, while the coal/biomass burning are increased due to more human activities. Both chemistry and emissions offer an explanation of the lower T/B ratios observed at 14:00 LT. In comparison with other months, higher T/B ratios were found more frequently in September, potentially showing increased industrial activities during this period.

Overall, based on the iso-pentane/i-pentane and T/B ratios, the atmospheric VOCs at every site were impacted by a mix of coal/biomass burning and vehicle emissions, whereas GS was more liable impacted by industry-related sources.

3.6 Relative reactivity of VOCs

The reactivity of individual species is different, and in mixtures of VOCs there is competition for reaction partners, leading to variations in reaction pathways and O_3 formation yields. Ozone formation potential (OFP) is a useful tool to estimate maximum O_3 productions of each compound under optimum conditions, from which the most important species for O_3 formation could be identified (Carter, 1994). The calculation of OFP is based on mixing ratios and maximum incremental reactivity (MIR) of each individual compound, Eq. (4).

$$OFP=C_i\times MIR \qquad (4)$$

where C_i represents the concentration level of i^{th} species, while *MIR* is a constant taken from (Carter, 2010) (Table S2).

In Zhengzhou city, alkenes contribute most ($55.9\pm14.2\%$) to the sum of OFP, of which ethylene had the largest portion. The results is different with the estimation based on emission inventories by Wu and Xie (2017), in which the largest contributor of total OFP in North China Plain (NCP), YRD and PRD was aromatics, reflecting

that there was relatively less surface coating industries in Zhengzhou.

For the individual species, the top 10 most contributors in OFP included ethylene, isoprene, m,p-xylene, toluene , propylene, acetylene, n-butane, i-pentane and propane. Their contributions to the sum of OFP was lied within the range of 69.4 - 77.6% (Table 5), with 61.3-76.5% of total VOCs weighted in concentration, highlighting the importance of reduction on emissions of these VOCs no matter based on relative reactivity or mixing ratios. Additionally, it is worth noting that, the percentage of acetylene (4.51±0.34%) weighted in OFP was higher than many other areas in China, including Guangzhou (2.20%) and YRD (2.37%) (Li and Wang, 2012; Jia et al., 2016), demonstrating that it is necessary to conduct emission controls on sources related to combustion (i.e., vehicle emissions and biofuel burning) in Zhengzhou city.

Zhengzhou was suffered from the severest O_3 pollution in June, 2017. The relationships between OFP of each organic group, $\Sigma_{VOCs,}$ and the ambient concentrations of NO_x and O_3, as well as the corresponding meteorological conditions, are shown in Fig. S5-6. At 07:00 LT, generally lower WS was seen than that at 14:00 LT, offered a favorite condition for local O_3 propagation. Under low RHs and high T and OFP (88.1±30.3 ppbv), the O_3 level at YH was unexpectedly lower than that at MEM on sunny days. Since the OFP was estimated with the assumption of reactions that proceeded under optimum conditions, the above phenomenon reflected there were unsatisfied O_3 formation conditions at YH. The highest total OFP was seen at JK in June, while the highest O_3 levels was observed at GS where located at a downwind position with lowest WS (0.74±0.33 m s^{-1}). The concentration level of O_3 usually increased with wind speed (Fig. S7), particularly when the eastern wind was dominant, illustrating the disturbance from long-distance sources to urban center.

3.7 Source apportionment

The factor profiles given by PMF for each site were presented in Fig. 15. The six factors were resolved as vehicle emissions, coal+biomass burning, solvent use, oil evaporation, petrochemical and biogenic source (detailed characterization can be referred to supporting information) on the base of the correspondent markers for each source categories, which were summarized in Table S7. Meanwhile, the correlation

coefficients, expressed in Pearson's *r*, were varied from 0.54 to 0.62 and 0.66 to 0.73 for SO_2 with coal+biomass burning, and NO_2 with vehicle emission, respectively (Fig. 16), proved the precise results gained in this study.

The weight percentage of each factor calculated with two criteria (absolute concentrations and OFPs) at the four sites were presented in Fig. 17. At every site, vehicle emission, coal+biomass burning and solvent use were the top three contributors to VOCs abundance in ambient air. Compared to JK and YH, even though the distances between thermal power plant and the observation site was the shortest at MEM, vehicle emission (36.8%) showed the largest portion instead. Coal+biomass burning (30.6%) had the highest contribution at GS, attributed to its downwind position and nearby suburbs that biomass burning occurred more frequently. The contributions from vehicle emission at the two urban centers of MEM (36.8%) and YH (37.4%) were comparable, but higher than those at JK and YH. The consumptions of solvent at GS (18.9%) and JK (14.9%) were higher than those at YH (10.1%) and MEM (11.5%), due to restriction on development of new industrial enterprises in urban center in recent years. Emissions from oil evaporation, petrochemical and biogenic emission were scarce, and their contributions were below 10% at every site.

On the base of O_3 formation impact, coal+biomass burning, solvent use, and vehicle emission were the three major contributors as well. In contrast to the concentration weighted method, the importance of solvent use estimated with OFP increased 28-65% for each site, and the significance of vehicle emissions decreased 29-53%. At YH and GS, small discrimination (< 4%) in contributions of coal+biomass burning between the two methods were found. On the other hand, the variations on coal+biomass burning at JK (a decline of 17%) and MEM (an increase of 29%) were more obvious, due to low abundance of reactive species in this factor at JK and high level of alkenes at MEM. Considering that the aging index of xylene/ethylbenzene was high at MEM (2.97) and low at JK (0.01) remarkably, demonstrating that the emission sources related to coal+biomass burning was fresher at MEM than JK.

Except for oil gas evaporation and biogenic sources, in which major emitted compounds with shorter life span, potential source regions for the other four identified sources (i.e., coal+biomass burning, vehicle emission, solvent usage and petrochemical) apportioned by PSCF method were presented in Fig. 18. Southwest of Shanxi province, western of Shandong province, and southwest of Henan province were identified as hot spots for the coal+biomass burning. The active emission areas for solvent use were concentrated in Henan province, and mainly located in southwest of Zhengzhou. The most contribution area for petrochemical was found in southwest of both Shanxi and Henan, northwest of Anhui, and southeast of Hubei provinces. For vehicle emissions, the strongest emission point was scattered in southwest of Henan, while Shandong, Anhui and Hubei provinces also distributed with strong emission points.

3.8 Consumption of VOCs and correlations with ozone level

The consumption of a VOC in the atmosphere could be presented as the difference from its initial mixing ratio and the observed value following an air parcel. In isolated stagnant air, the rate of change of VOC concentrations will be the sum of emissions, deposition, and chemical production and loss processes.

The average value of VOC consumption at urban center (MEM and YH, 4-6 ppbv) was lower than that in outer areas (JK and GS, 9-11 ppbv), and the average increment of O_3 at 14:00 LT was higher than that at 07:00 LT in marginal area, suggesting more efficient photochemical reactions at JK and GS. Meanwhile, the average values of $[\bullet OH]\Delta t$ for each site, ranked in the same order with VOCs consumption, were varied in a range of 2.9×10^{10} to 4.7×10^{10} cm^{-3} s. The values were slightly lower than the results of 4.9×10^{10} cm^{-3} s measured at Beijing in August-September, 2010 (Yuan et al., 2012), indicating that comparatively less aging process in Zhengzhou.

Taken the decrement of VOCs and NO_x as independent variable and the increment of O_3 as dependent variable, the multiple regression analysis was performed. The results for JK and GS were presented as:

$$[O_3]_{increment}=0.41[VOC]_{decrement}+0.20[NO_x]_{decrement}+53.4 \text{ (JK, } R^2=0.44)$$

656 $[O_3]_{increment}=0.34[VOC]_{decrement}+0.39[NO_x]_{decrement}+59.3$ (GS, $R^2=0.38$)

657 The F values for JK and GS were 16.1 and 10.1 respectively, indicating the
658 regression results at the two sites were acceptable. However, the relationships among
659 O_3, NO_x and VOCs could not be expressed in this way at MEM and YH, where the
660 low values for both R^2 (0.12, 0.09) and F values (2.7, 2.8). This potentially attributed
661 to more constant disturbance from fresh emission sources at urban center.

662 **4. Conclusions**

663 In this study, VOC samples were collected at four sites in Zhengzhou, Henan
664 (China) for the first time and analyzed for 57 species. It is found that the weighted
665 percentage of aromatics was lower, while alkyne was higher in Zhengzhou city than
666 in other Chinese cities. C_2 - C_5 alkanes, acetylene, ethylene, toluene and benzene were
667 the most abundant VOCs in the region, suggesting widespread combustion-related
668 sources in the city. Median concentrations for the four sites are almost
669 indistinguishable but, based on monthly averages, the maximum Σ_{VOCs} was observed
670 at GS site, because it is occasionally impacted by emissions from the nearby gas
671 fueled plant, which strongly skew the distribution of measured VOC concentrations.
672 Approximately 75% of VOCs/NO_x ratios were below 6 at each site, indicating that the
673 O_3 formation was driven by VOCs regionally. Different from other megacities,
674 alkenes were the biggest contributors to OFP, and acetylene was particularly critical at
675 each site. In addition, the impact of aging process was less in Zhengzhou than that
676 Beijing. Photochemical processing appears to be more efficient at JK and GS, while
677 the relationships among O_3, NO_x and VOCs at urban sites of MEM and YH were
678 more complex.

679 Our analysis of ozone formation does not take into account the important effects
680 of transport and mixing, and should be viewed in this light. Both measured mixing
681 ratios and calculated OFPs demonstrated that the most important contributors to
682 VOCs were vehicle exhaust, coal+biomass burning and solvent use, illustrating the
683 necessary to conduct emission controls on these pollution sources. Vehicle emission
684 was more dominant at urban center (YH and MEM), while solvent use was more
685 important at the sites (JK and GS) far away from urban center in Zhengzhou. It is

686 further shown that the air pollution in Zhengzhou was usually impacted by local
687 emissions, with no more than 50% of 48-hour backward trajectories extended out of
688 Henan province in June, August and September, and southern air clusters occasionally
689 from Hubei Province was cleaner. In addition, strong emissions for coal+biomass
690 burning were concentrated in southwest of Shanxi, western of Shandong and
691 southwest of Henan provinces according to the PSCF analysis. Due to less
692 anthropogenic emissions and more favorable dispersion conditions, most of the air
693 pollutants had the lowest levels in the mid-summer month of July. This study provides
694 the first-hand information on the characteristics of VOCs and assists in overcoming
695 the O_3 pollution issue in Zhengzhou city, China.

696 **Acknowledgements**

697 The authors would like to thank for valuable suggestions, corrections, and
698 discussions from both anonymous referees and editor, Prof. Rob MacKenzie. Their
699 comments are particularly important and greatly contributed to improve this work.
700 This research was supported by the Key Program of National Natural Science
701 Foundation of China (Grant No. 91744209).

Table & Figure

Table 1. Mean concentrations of Σ_{VOCs} (ppbv) and correspondent standard deviations (SD) at every site during the sampling period

	JK		MEM		GS		YH	
	Mean	**SD**	**Mean**	**SD**	**Mean**	**SD**	**Mean**	**SD**
May.2017	37.6	22.6	29.3	15.3	31.7	18.7	30.1	16.4
June.2017	34.0	19.9	30.3	12.8	39.3	25.4	28.3	11.9
July.2017	16.0	6.1	20.7	12.7	19.6	13.9	15.9	7.5
Aug.2017	21.5	15.3	24.4	20.8	20.5	15.7	26.1	17.0
Sept.2017	26.2	16.2	34.2	23.8	30.4	19.8	32.6	19.8

Table 2. Wind speed (m s^{-1}) measured about 10m above ground level at every site during the sampling period

	JK	**MEM**	**YH**	**GS**
May	1.34±0.65	1.86±1.19	1.27±0.66	0.97±0.49
June	1.07±0.48	1.86±0.94	0.97±0.36	0.74±0.33
July	1.48±0.59	2.62±1.19	1.15±0.45	0.90±0.32
August	1.06±0.48	1.86±0.94	0.95±0.39	0.76±0.35
September	0.80±0.38	1.24±0.80	0.82±0.43	0.62±0.38

710 Table 3. Concentration levels of VOCs and compositions of major groups in Zhengzhou and other

711 cities in China

Items		**Guangzhou**	**Nanjing**	**Beijing**	**Hangzhou**	**Wuhan**	**Zhengzhou**
		March-December, 2005	2011-2012	August, 2006	July-August, 2013	2013-2014	May-September, 2017
Sampling site		residents-commercial-transportation mixed area	transportation-industry mixed area	residents-commercial mixed area	residents-transportation mixed area	urban	urban
Quantified compounds		59 NMHC	56 NMHC	47 NMHC	56 NMHC	99 VOCs	56 NMHC
Total samples		145	_	24	_	_	400
TNMHC (ppbv)		47.3	43.5	65.6±17.4	55.9	23.3±0.5	29.2±23.1
Compositions of major groups (%)	*alkane*	49.0	45.0	52.3	33.2		56.7±12.4
	alkene	16	25.3	21.2	25.9		16.2±7.6
	aromatic	23	22.3	18.1	24.3		14.1±8.4
	alkyne	12	7.3	8.4	16.6		12.9±6.7
Reference		(Li and Wang, 2012)	(An et al., 2014)	(Guo et al., 2012)	(Li et al., 2017b)	(Lyu et al., 2016)	this study

712

713

714

715

716

717 Table 4. Specific information on VOCs, O_3 and NO at the four sites in June, 2017

Composition or conc.	JK	MEM	YH	GS
Aromatic (%)	9.06	11.6	4.72	15.8
Alkene (%)	6.36	4.13	5.52	5.47
Σ_{VOCs} (ppbv)	34.0	30.3	28.3	39.3
O_3 (ppbv)	74.9	73.5	73.8	88.0
NO (ppbv)	7.10	7.72	2.34	4.47

718

719 Table 5. Top 10 VOCs ranked according to calculated ozone formation potential (OFP) and their

720 corresponding percentage weighted in mixing ratio

Site	Species	OFP (ppbv)	Weighted in OFP (%)	Weighted in mixing ratio (%)	Site	Species	OFP (ppbv)	Weighted in OFP (%)	Weighted in mixing ratio (%)
JK	Ethylene	19.0	25.5	8.22	MEM	Ethylene	18.4	30.9	7.92
	Isoprene	13.0	21.8	7.31		Isoprene	4.66	10.1	2.36
	m/p-Xylene	6.08	5.89	2.67		Toluene	3.73	6.67	3.99
	Toluene	5.53	5.83	4.22		Propylene	3.60	6.16	1.25
	Propylene	4.03	5.36	1.29		Acetylene	2.82	5.00	12.2
	Acetylene	2.97	4.44	13.5		m/p-Xylene	2.55	4.20	1.40
	n-Butane	2.15	3.05	7.28		n-Butane	1.81	3.20	5.97
	o-Xylene	1.83	2.00	0.88		Isopentane	1.76	3.16	7.39
	Isopentane	1.66	1.95	6.50		Ethane	1.58	2.96	23.4
	Propane	1.17	1.73	9.77		Propane	1.31	2.48	10.6
YH	Ethylene	19.8	28.1	8.88	GS	Ethylene	18.1	26.90	7.51
	Isoprene	7.44	11.3	3.67		Isoprene	8.01	16.8	4.64
	Toluene	6.63	7.75	5.72		Toluene	7.43	7.67	5.49
	m/p-Xylene	3.93	4.38	1.58		Propylene	4.39	5.85	1.26
	Acetylene	3.15	4.38	13.9		m/p-Xylene	4.31	4.57	1.75
	Propylene	3.01	3.60	0.91		Acetylene	2.76	4.24	12.1
	Trans-2-pentene	2.25	2.94	3.43		n-Butane	1.82	2.93	6.39
	n-Butane	1.84	2.80	6.31		Isopentane	1.71	2.68	6.94
	Isopentane	1.59	2.22	6.69		Propane	1.38	2.26	11.6
	Propane	1.18	1.98	10.2		Isobutane	1.13	1.98	4.59

721 [a] *m*-Xylene and *p*-Xylene are co-eluted in the chromatographic separation.

722

723

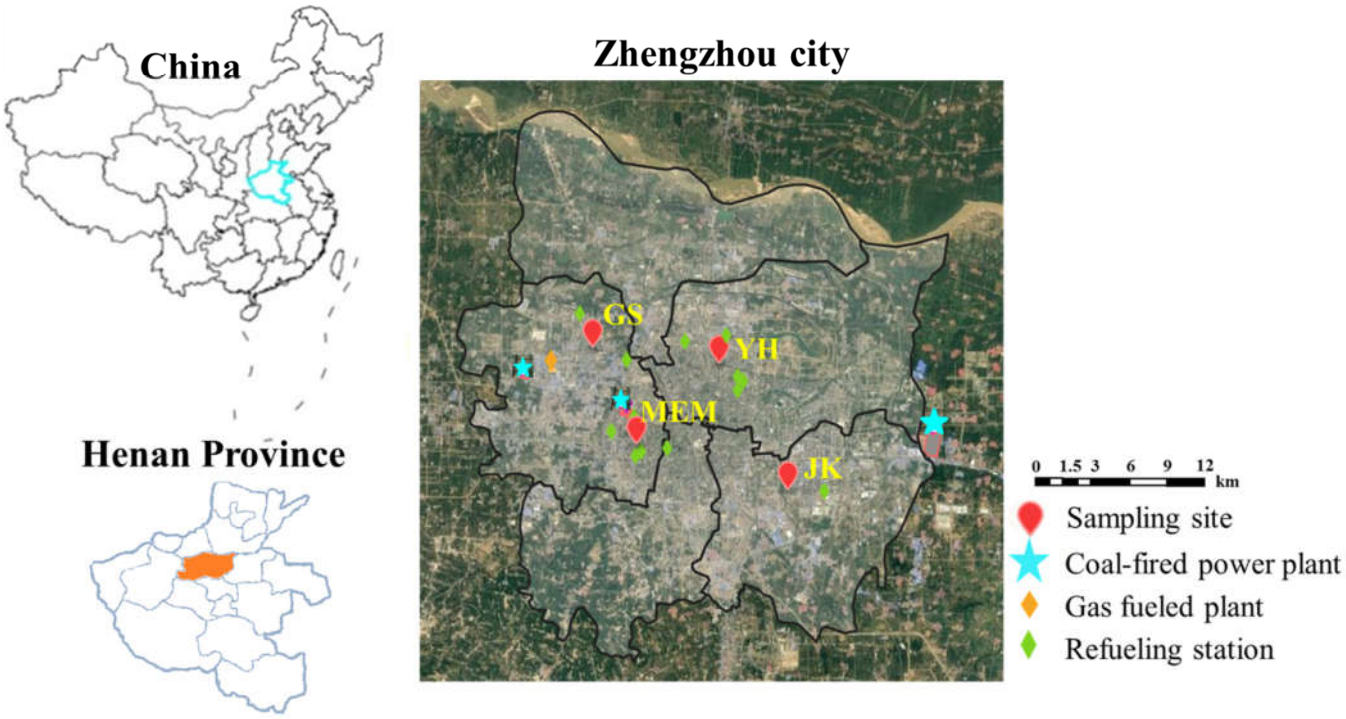

724

725 Fig. 1. Satellite imagery showing the four sampling sites and surrounding areas of Zhengzhou,

726 China, including major emission sources presented with different marks

727

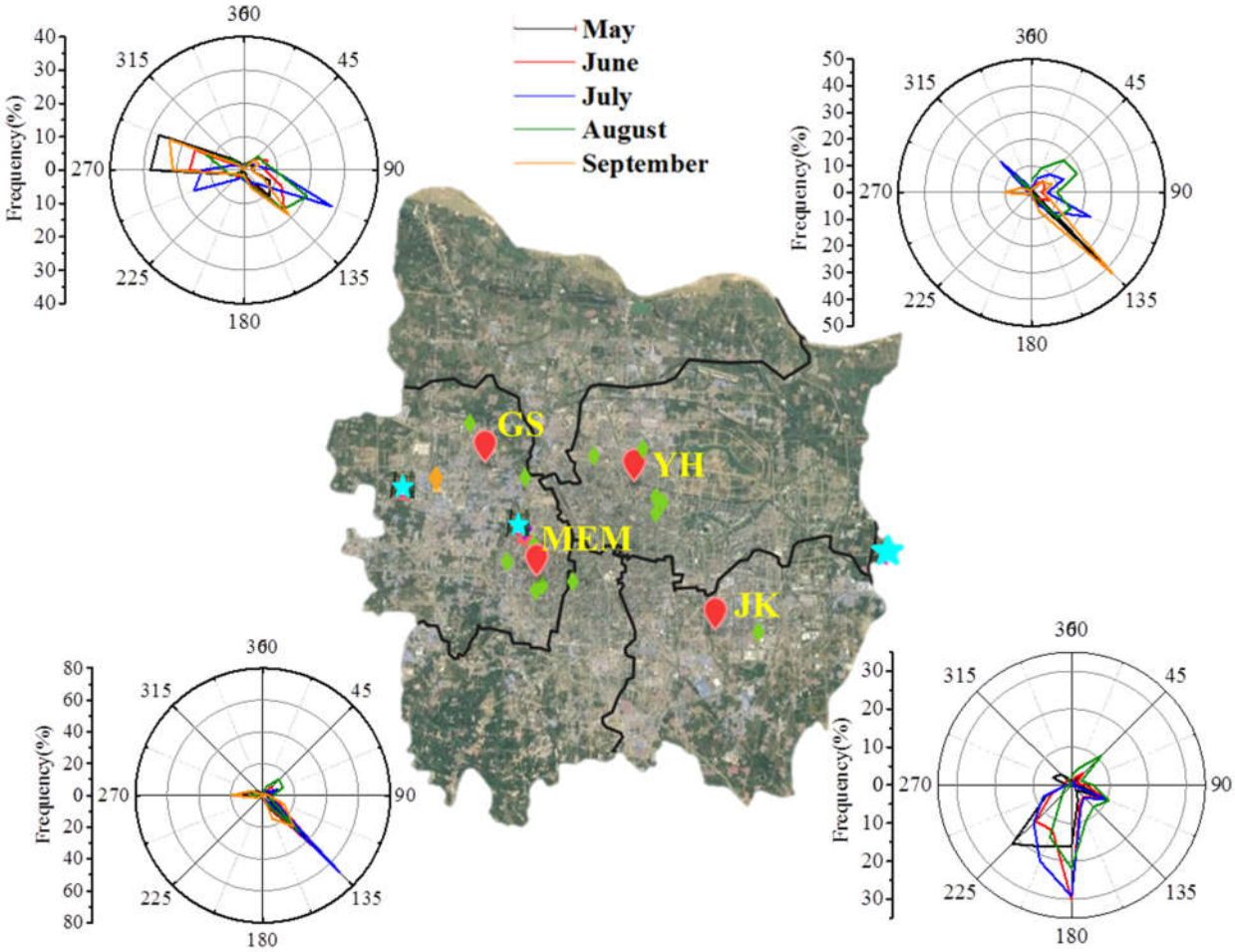

Fig. 2. Wind direction for each site during May to September, 2017

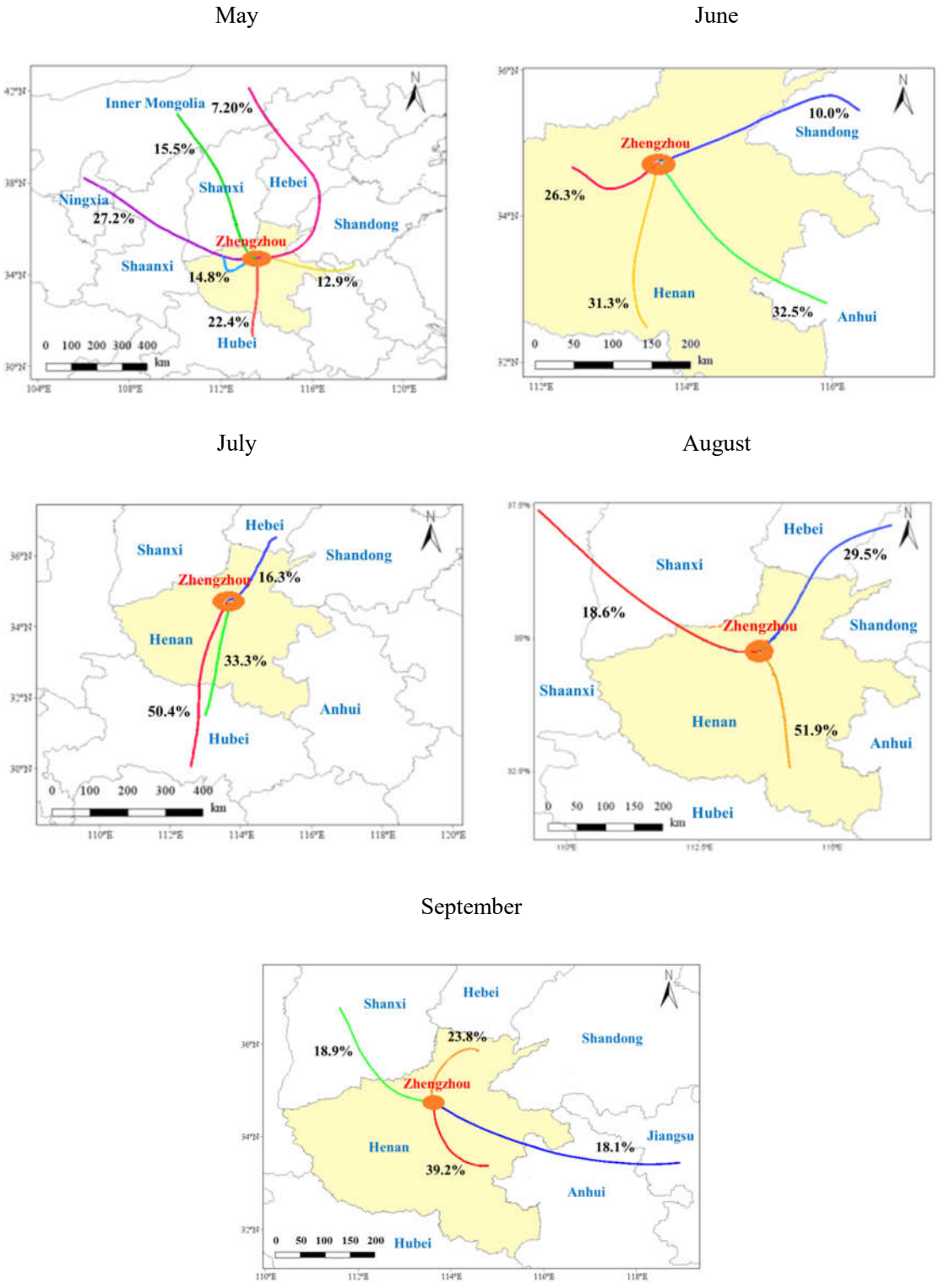

731 Fig. 3. Cluster analysis of 48-hour backward trajectories for Zhengzhou in each sampling month
732 using HYSPLIT code, with the start height at 500m altitude and running interval set as 2- hour for
733 each day, percentage of each cluster and covered areas are presented as well.

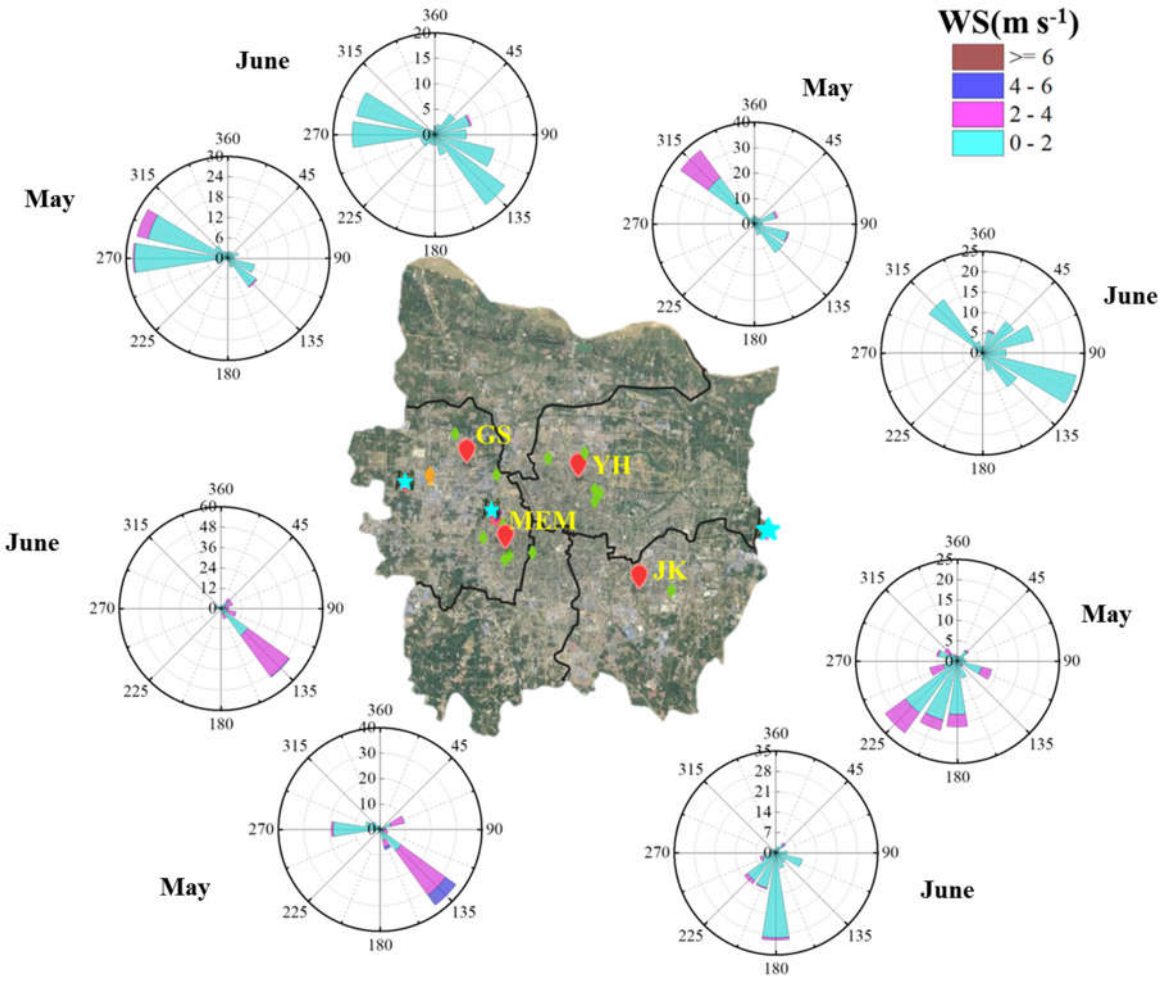

734

735 Fig. 4. Wind rose plot showing wind sector frequency (%) of occurrence and associated wind

736 speed (m s^{-1}) at each site in May and June (the wind distribution in other three months were

737 illustrated in Fig. S2), which were recorded by the anemometers placed at the same site with other

738 air monitors.

739

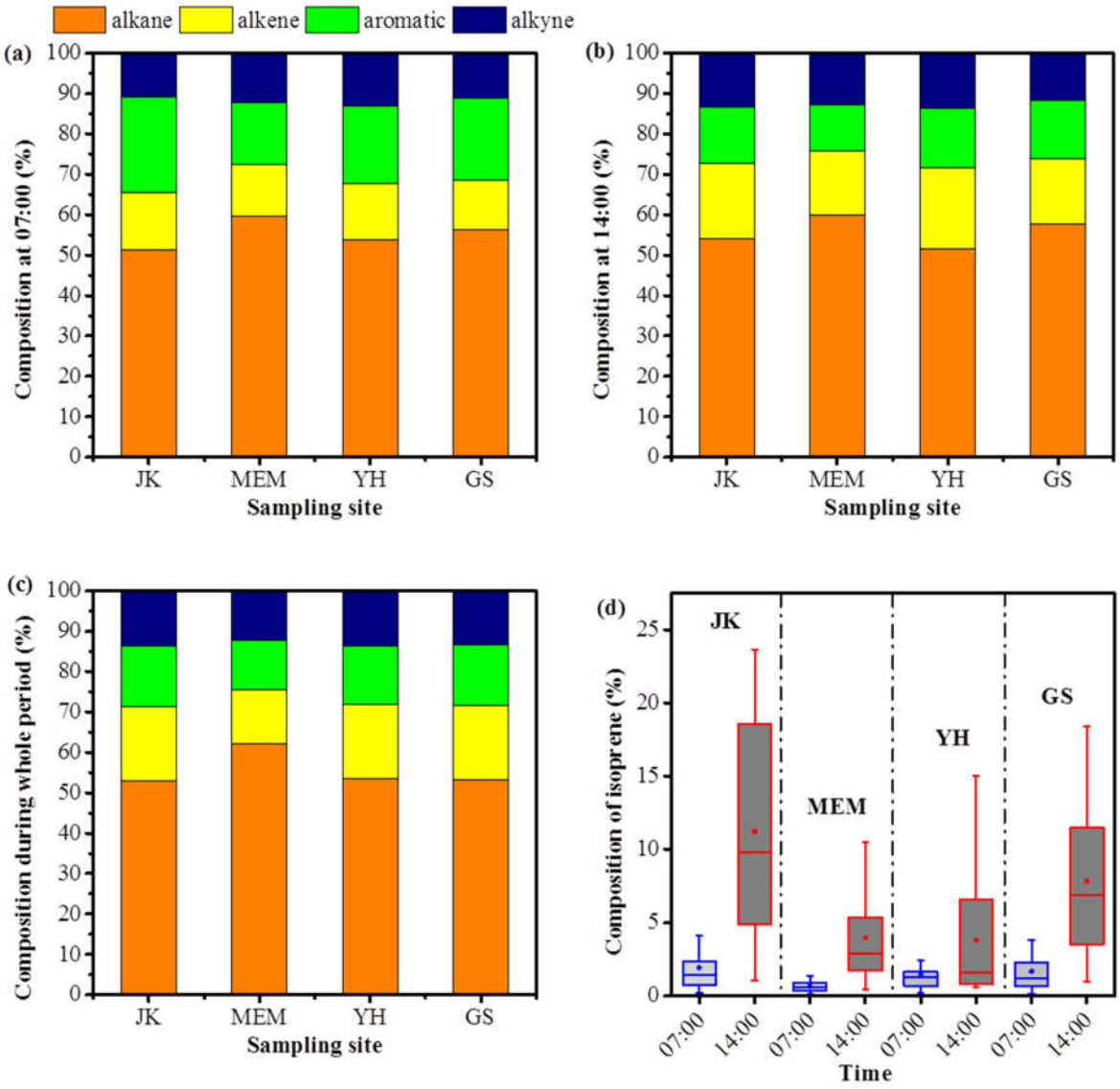

Fig. 5. Compositions of major organic classes at 07:00 LT (a), 14:00 LT (b) and during the whole sampling period (c) at the four sites, and the box plot for the composition of isoprene at 07:00 LT and 14:00 LT for each site, with the whiskers range in 5-95%iles, and the box shows the 25-75%iles, the solid dots represents the arithmetic average, the line in the box shows the median (d).

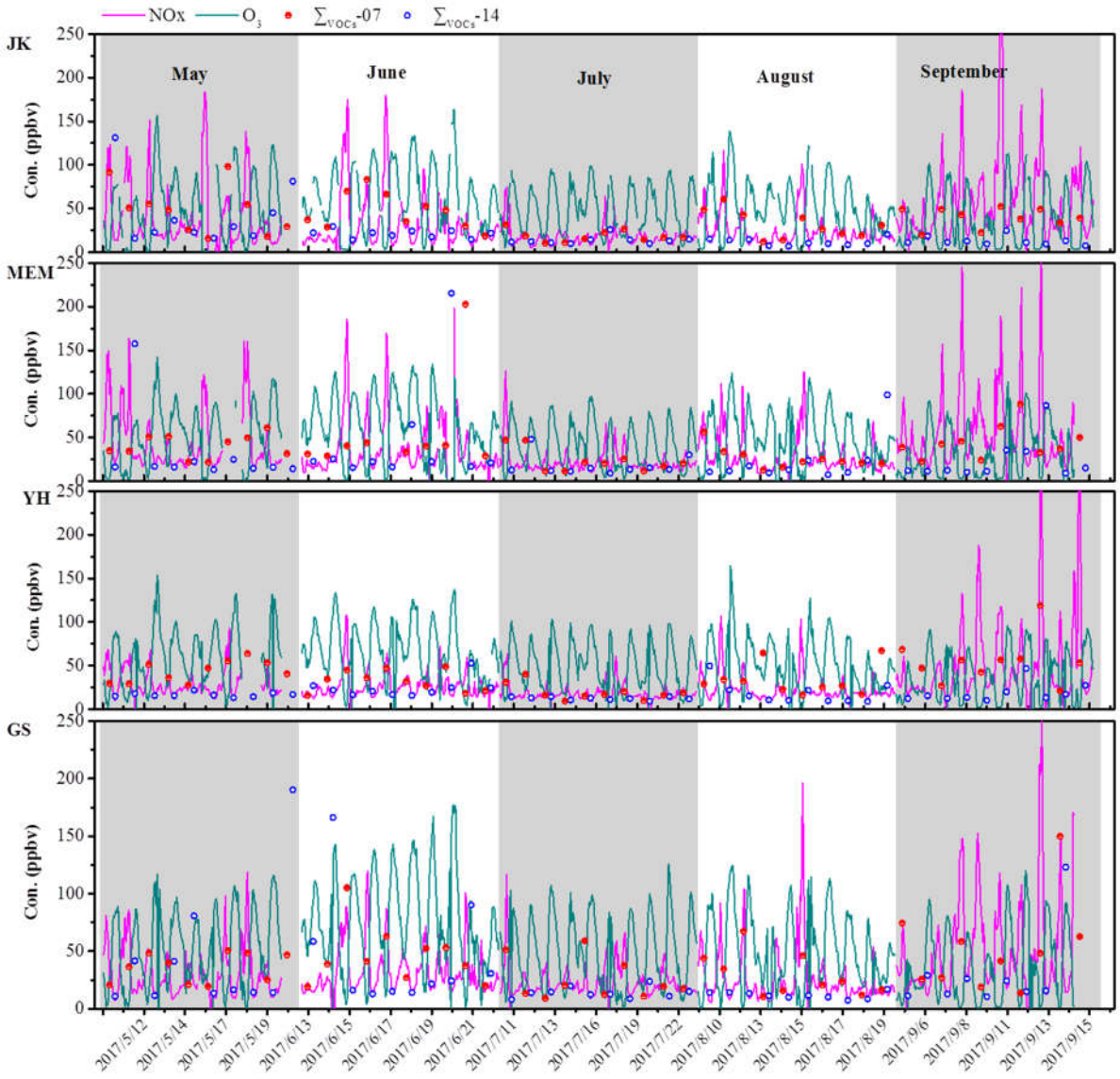

Fig. 6. Temporal variations of mixing ratios of Σ_{VOCs}, NO_x and O_3 at the four sites during the whole sampling period, in which Σ_{VOCs}-07 stands for the concentration level of Σ_{VOCs} observed at 07:00 LT, and Σ_{VOCs}-14 was that observed at 14:00 LT.

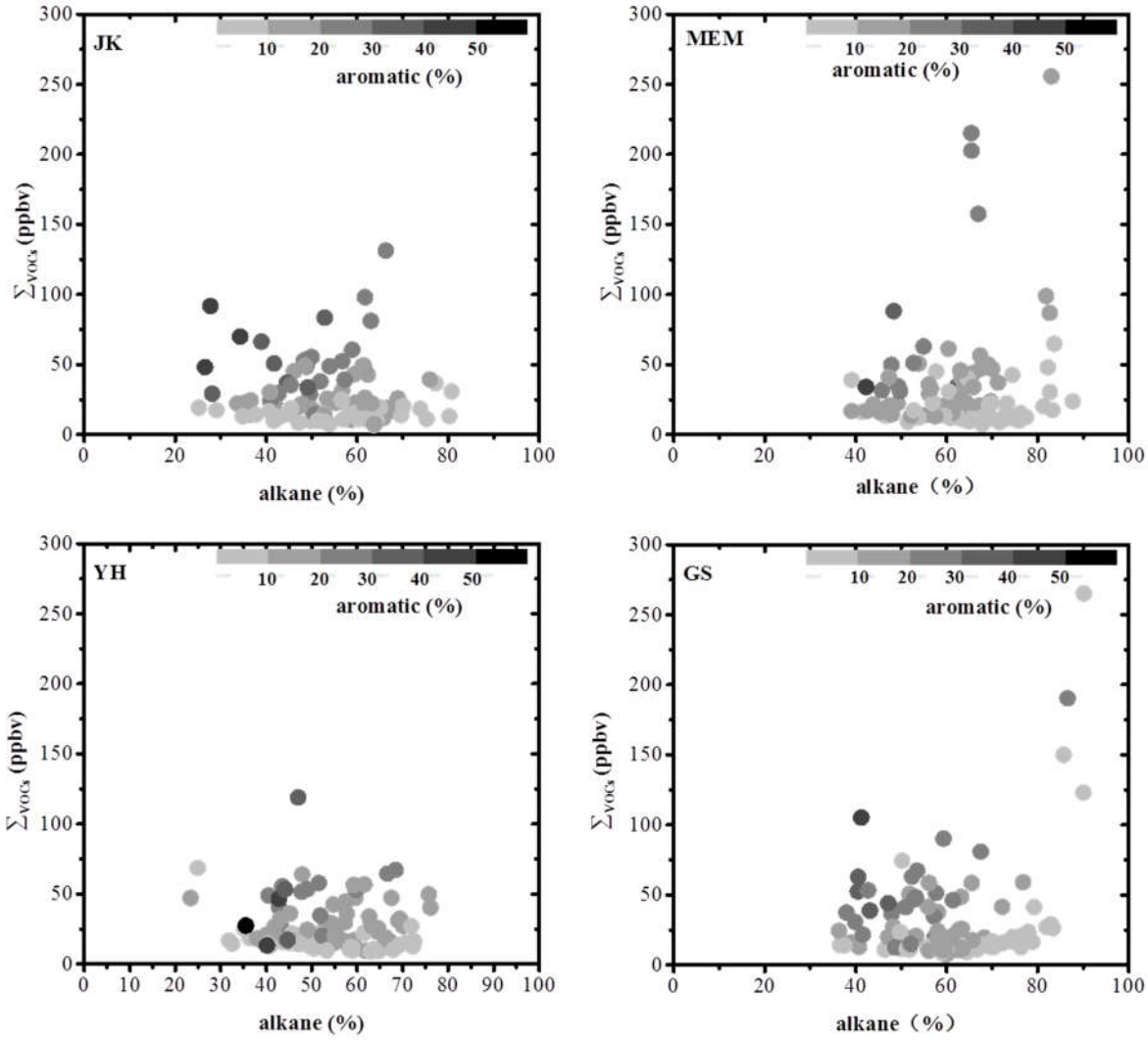

Fig. 7. The relationship between mixing ratio of Σ_{VOCs} and the composition of alkane, the data points are color coded with the composition of aromatic.

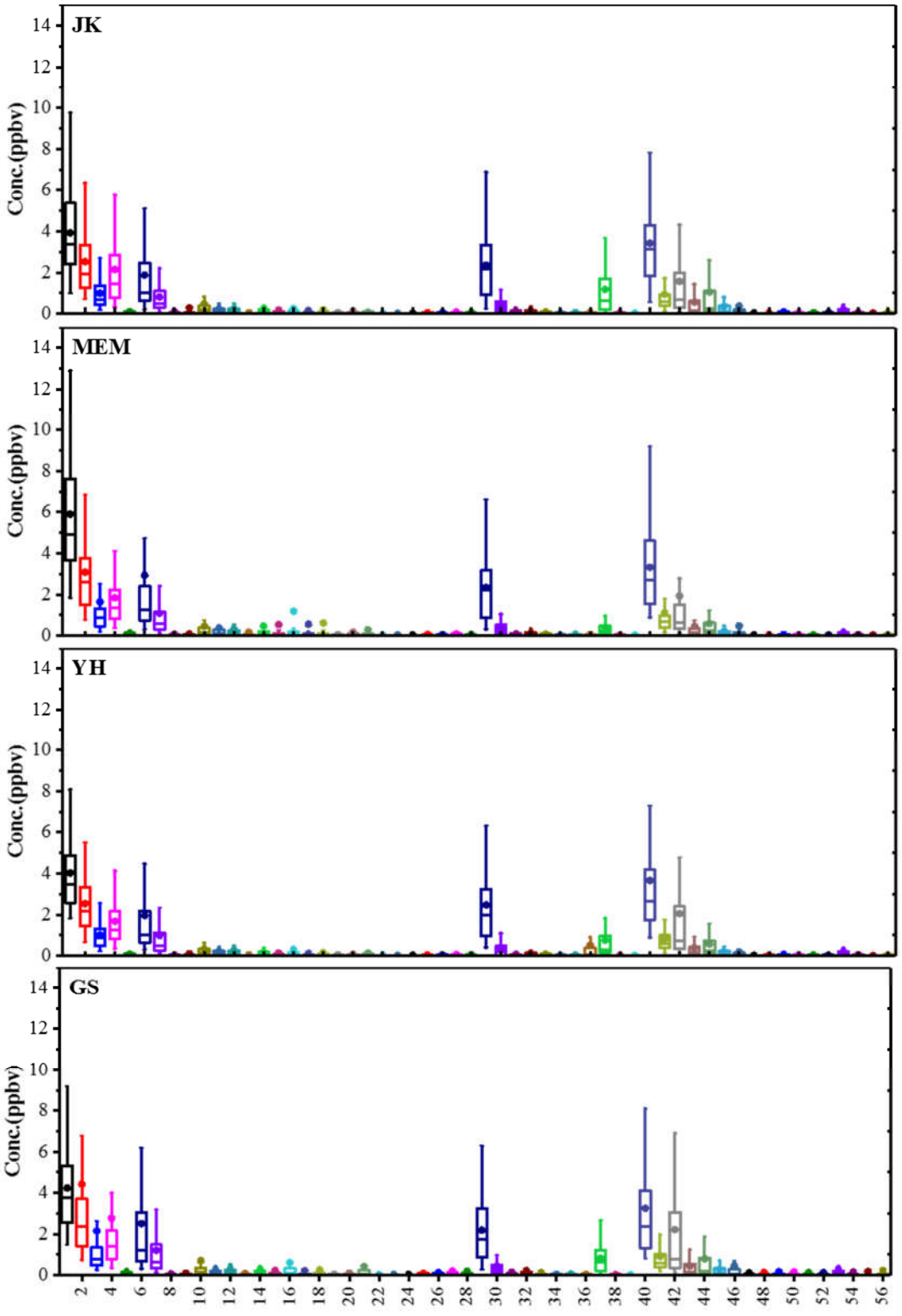

760

761 Fig. 8. Concentrations of 57 VOCs at each site for the whole sampling period, the whiskers show

762 the 5-95%iles, and the box shows the 25-75%iles, the solid points shows the arithmetic average,

763 the line in the box shows the median. The chemicals are listed in Table S1.

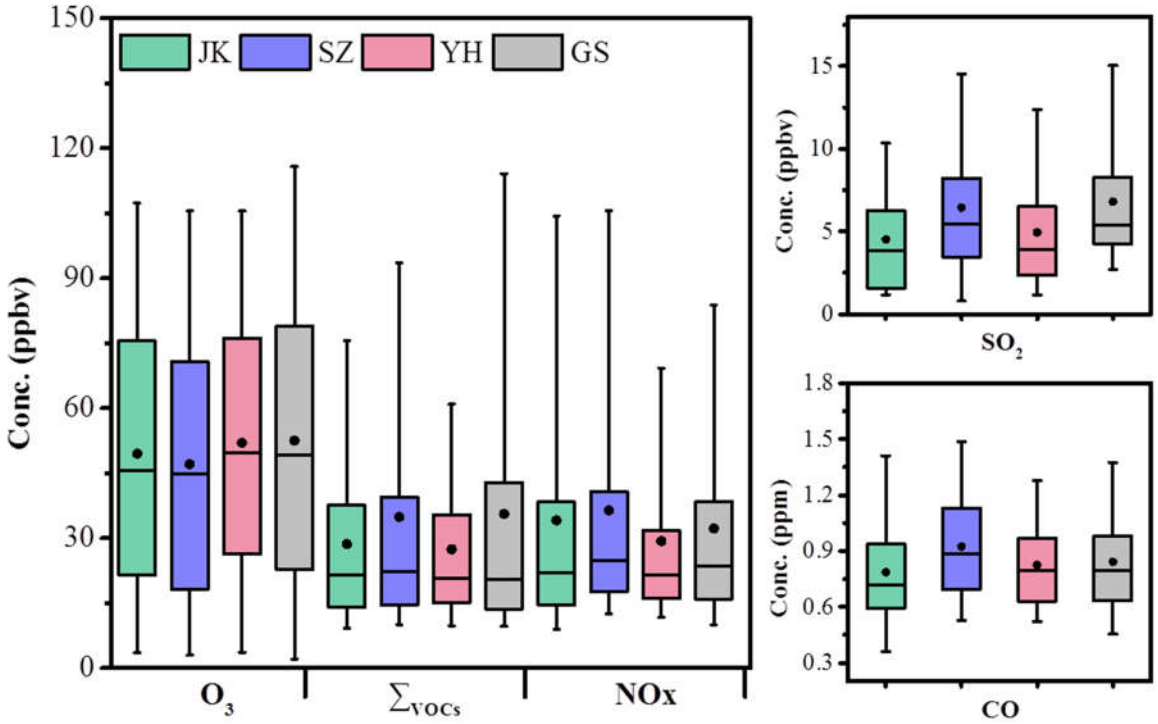

764

765 Fig. 9. The distribution of concentration point on O_3, Σ_{VOCs}, NO_x, SO_2 and CO at each site, the

766 range of the box was 25%-75%, the black line in the box stands for median level, the black dot

767 represent the average level, the range of whisker was 5-95%.

768

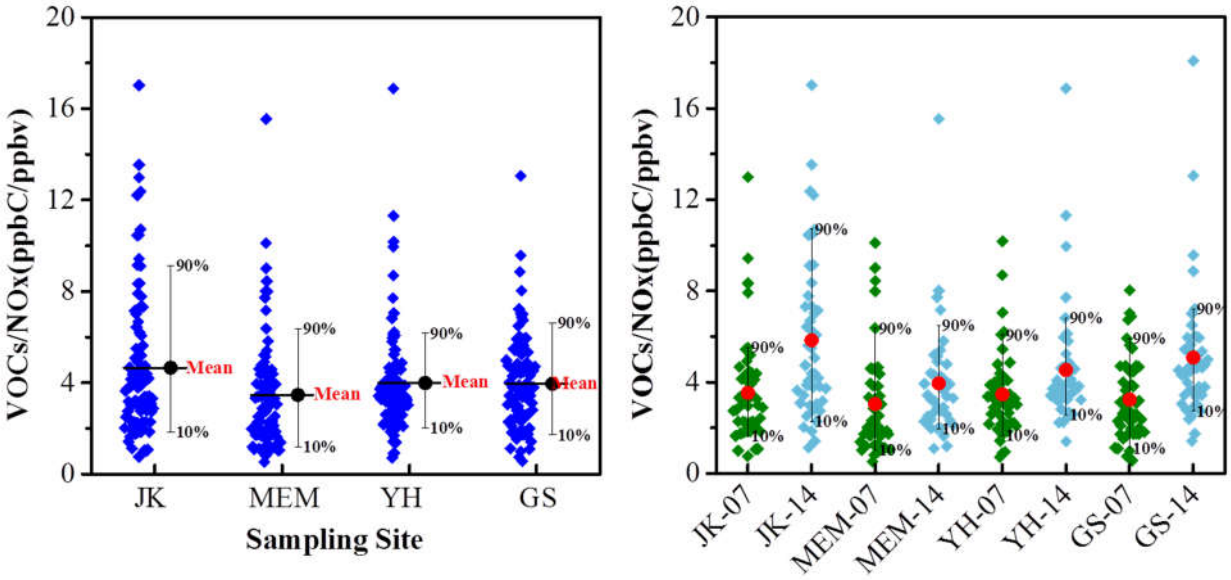

769

770 Fig. 10. The data distribution of VOCs/NO_x(ppbC/ppbv) at the four sites (left), and the ratio

771 observed at 07:00 LT and 14:00 LT were presented (right).

772

773

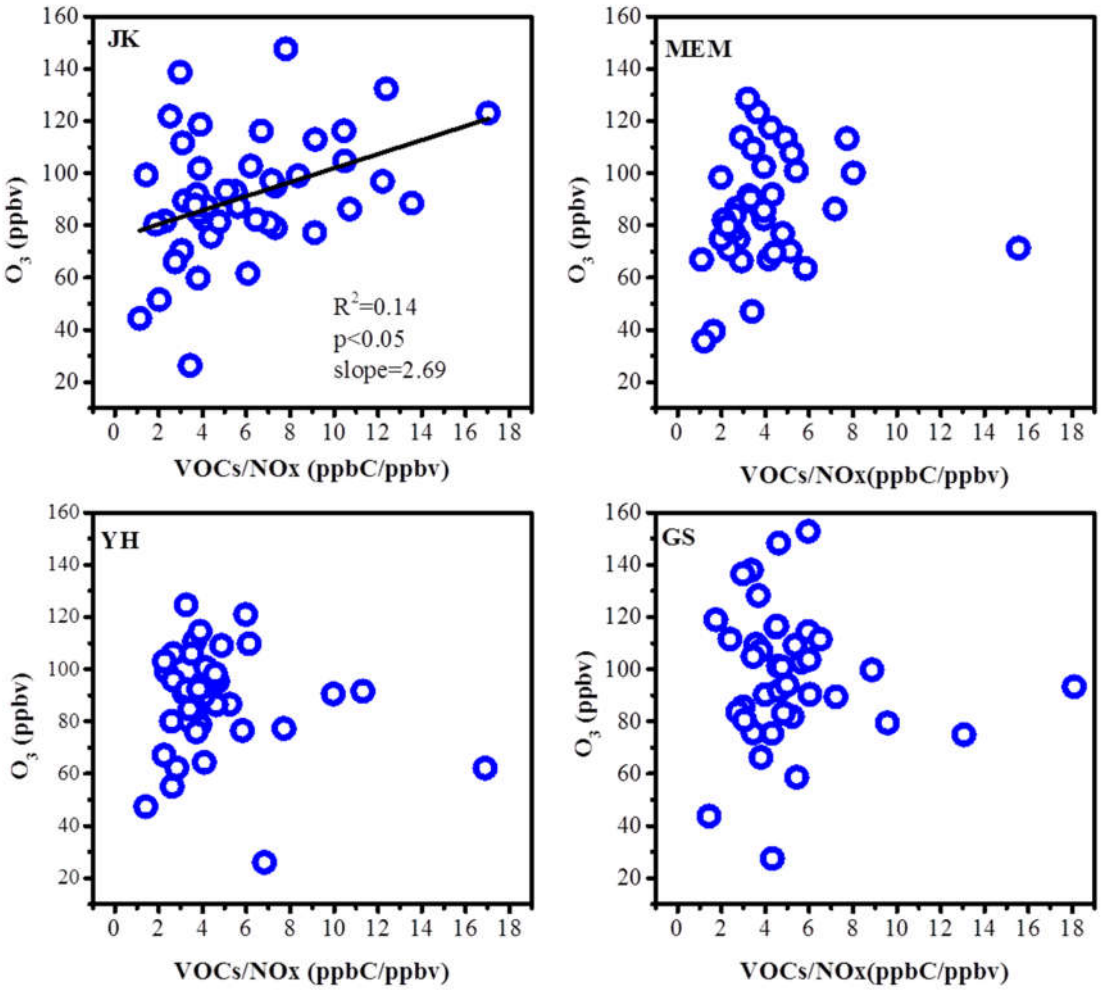

Fig. 11. The relationship between O_3 and VOCs/NO_x at 14:00 LT for each of the four sampling sites.

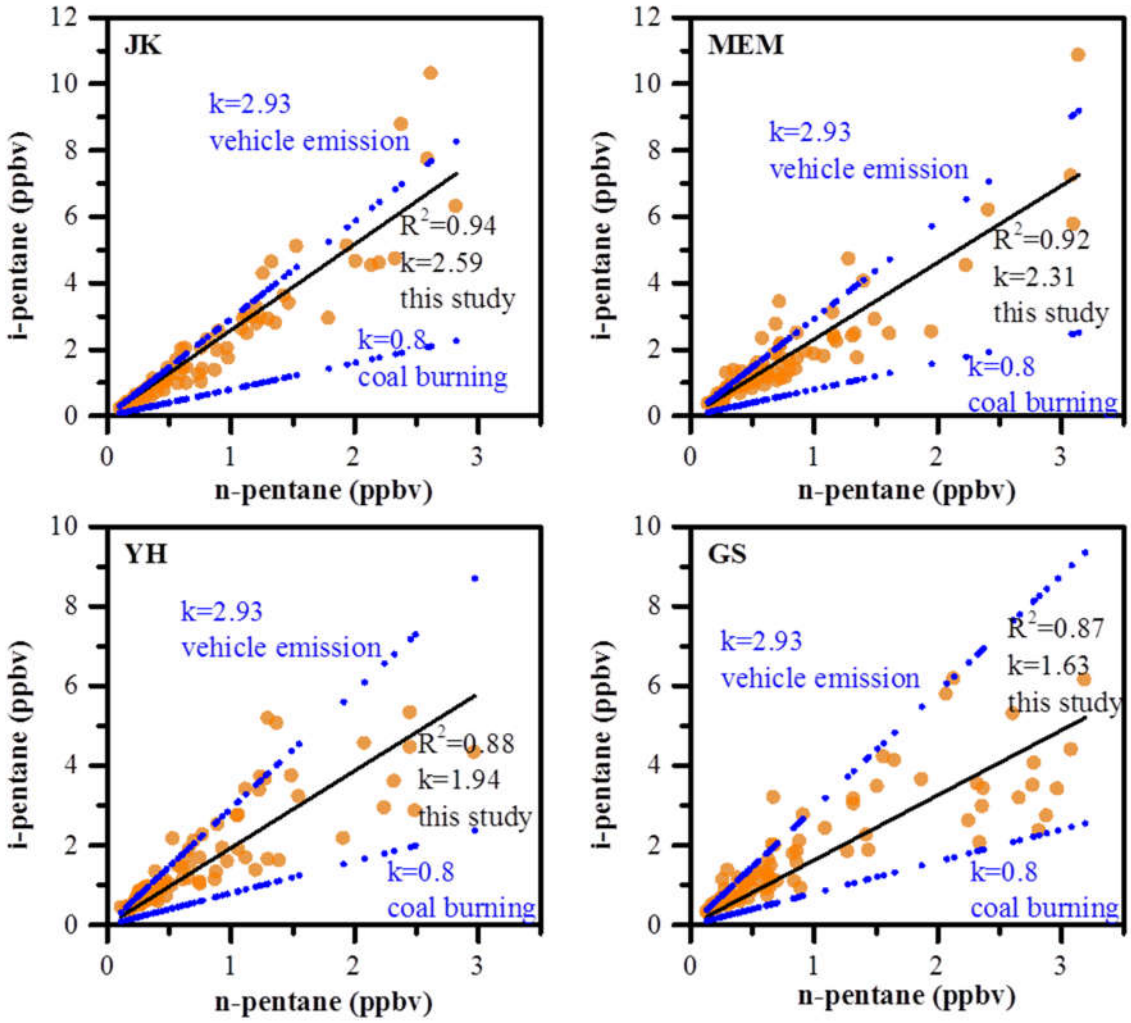

781

782 Fig. 12. Ratios of isopentane to n-pentane at every site

783

784

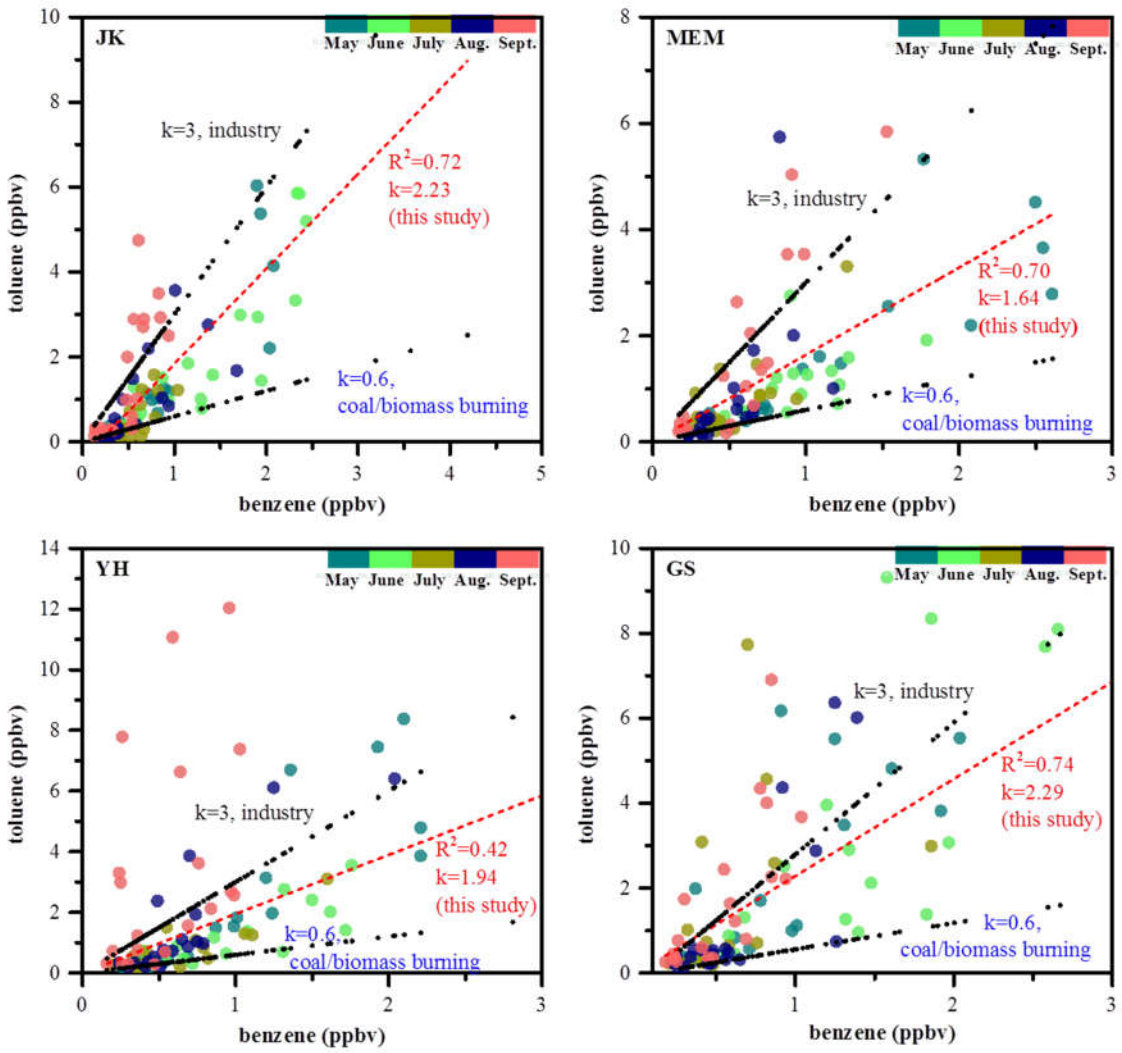

785

786 Fig. 13. T/B ratios and linear correlation coefficients (R^2) between benzene and toluene at every site,

787 the data points were color mapped with sampling period.

788

789

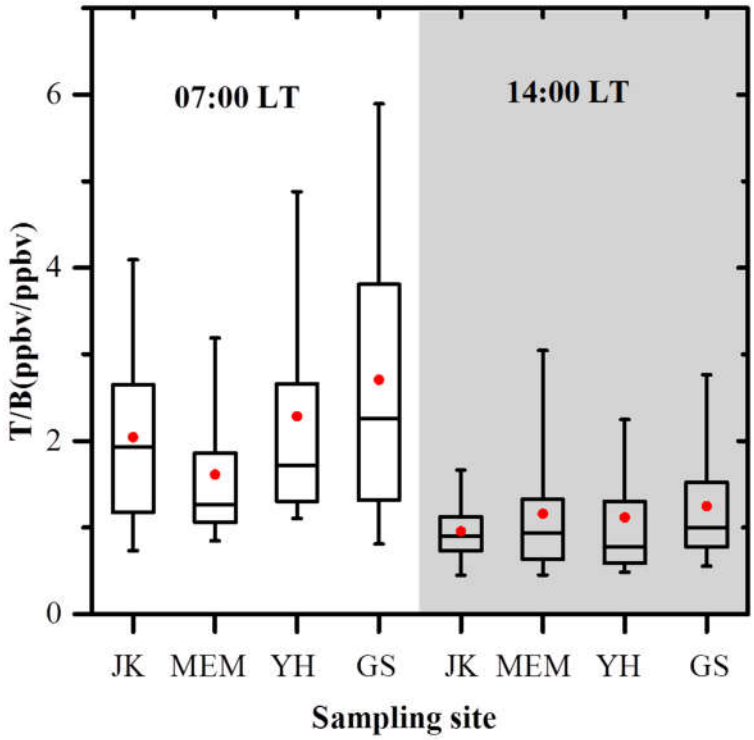

Fig. 14. The average ratio of T/B at 07:00LT and 14:00LT for each site during the whole sampling period

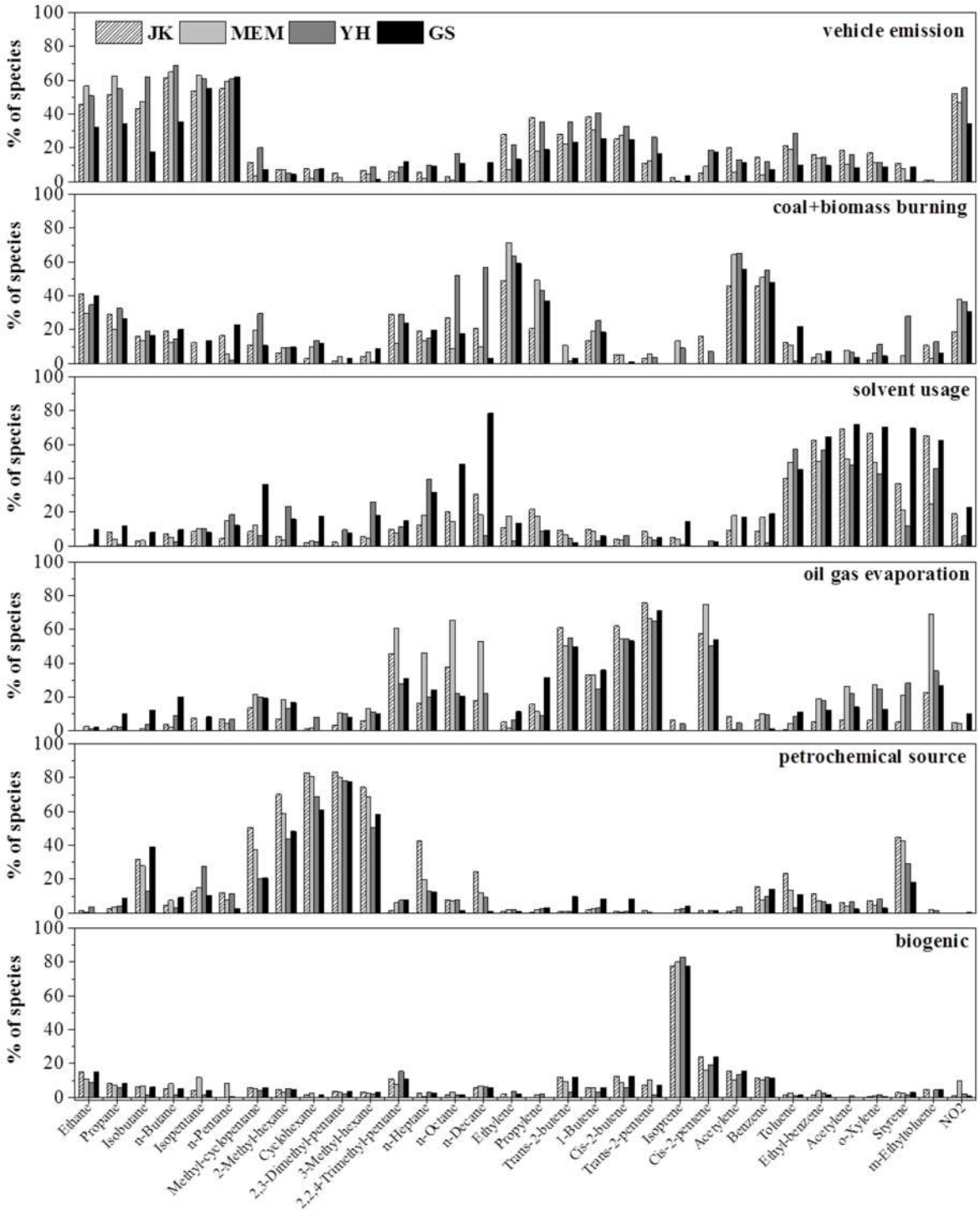

Fig. 15. Factor profiles of major emission sources, namely vehicle emission, coal+biomass burning, solvent usage, oil gas evaporation, petrochemical and biogenic source resolved by positive matrix factorization (PMF) model.

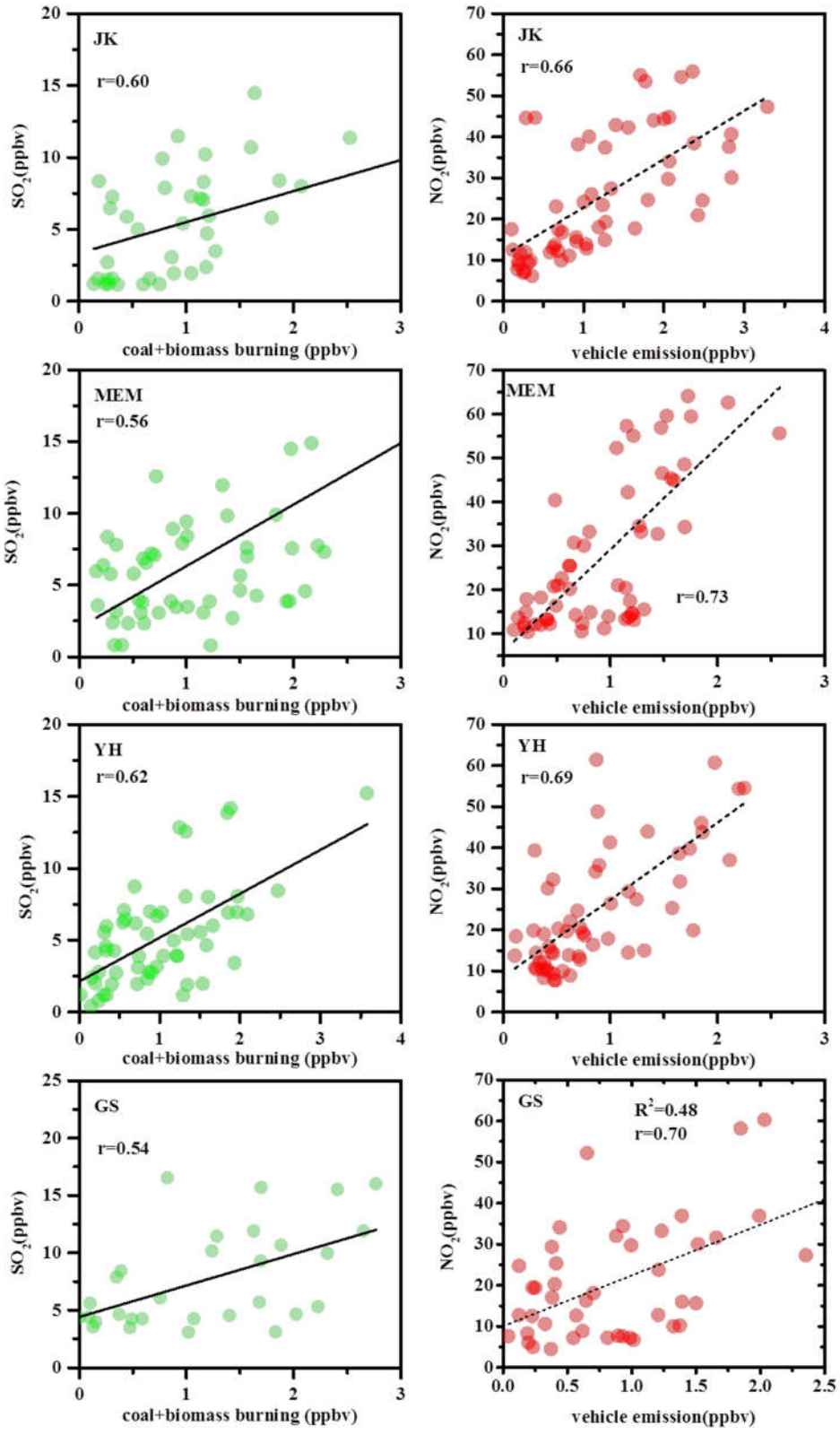

800

801 Fig. 16. Correlation analysis relating source-apportioned VOC contributions of coal+biomass

802 burning (left column) and vehicle emission (right column) with co-located measurements of SO_2

803 and NO_2 for each site (rows).

804

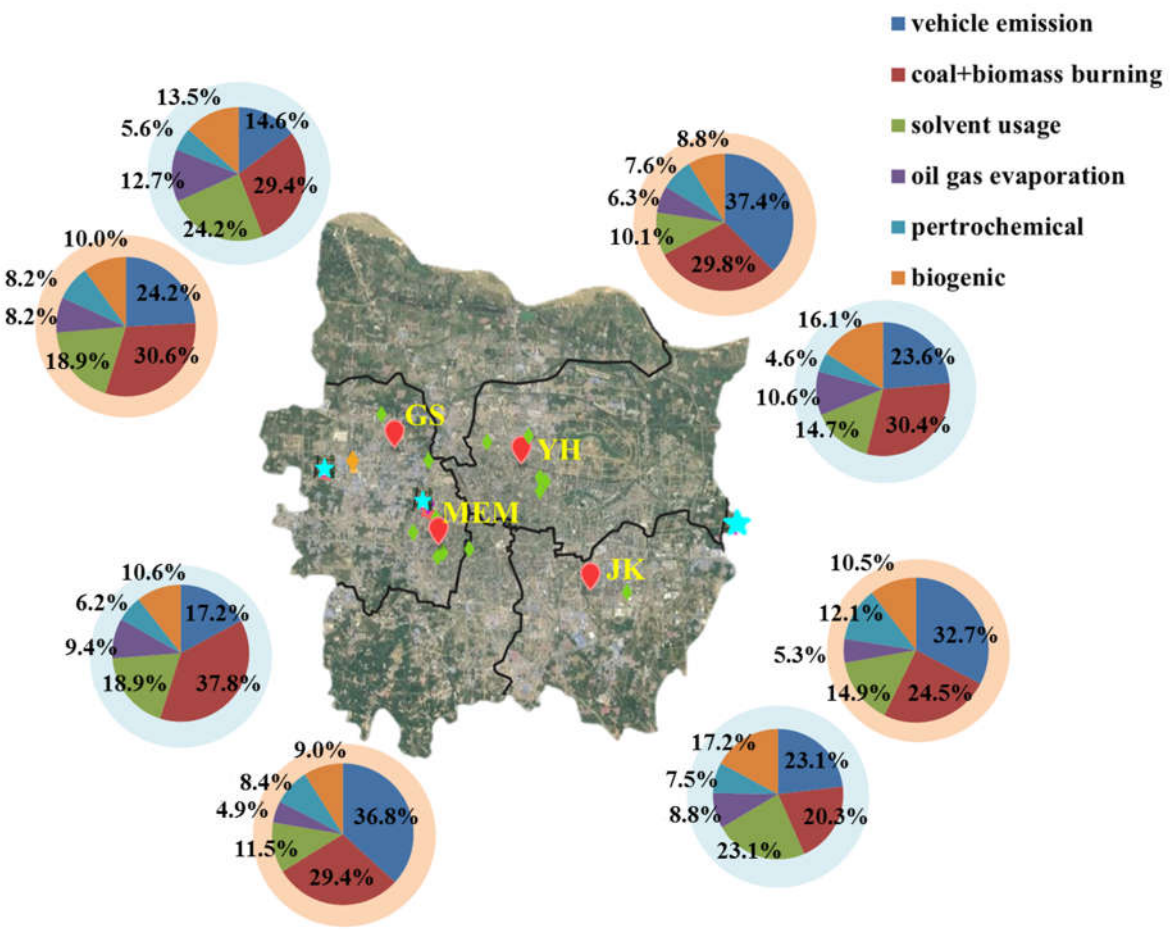

Fig. 17. Source apportionment results during the whole sampling period. The results weighted in observed concentrations were shadowed with pink color, and the results estimated based on OFP were shadowed with light blue color.

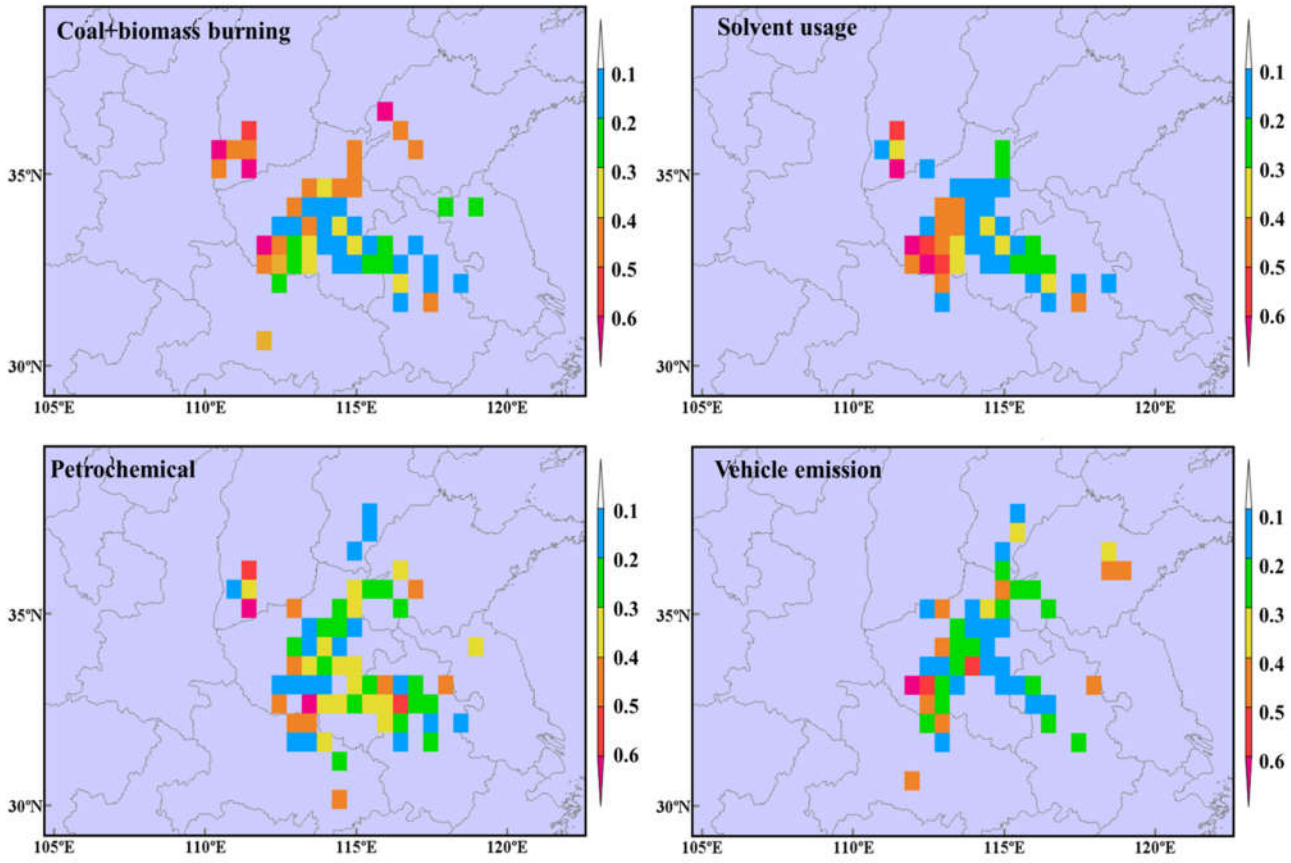

Fig. 18. Probable source regions apportioned by PSCF at Zhengzhou at summer (June-Aug. 2017) during sampling period